Polymer Chemistry

ROYAL SOCIETY OF CHEMISTRY

REVIEW

View Article Online
View Journal | View Issue

Cite this: *Polym. Chem.*, 2020, **11**, 3095

Fluorescent chemosensors based on conjugated polymers with N-heterocyclic moieties: two decades of progress

Taisheng Wang,[a,b] Na Zhang,[a,b] Wei Bai[c] and Yinyin Bao *[d]

Among various fluorescent chemosensors based on different platforms, π-conjugated polymer-based sensors have attracted much attention, owing to their amplified detection sensitivity in the detection of a variety of environmental pollutants and bioactive compounds. Since the report of the first conjugated polymer sensor in the 90s, this sensing platform has achieved more than two decades of progress, with an explosion of the research in this field observed in the last ten years. In this review, we will focus on fluorescent polymer sensors with N-heterocyclic aromatic moieties, which have played a pivotal role since the beginning of the development of the conjugated polymer-based fluorescence sensing strategy. We will highlight the representative examples according to the different types of heterocycles, illustrate the structure–property relationships, point out the limitations and challenges of current systems, and also identify possible future research directions.

Received 1st March 2020,
Accepted 22nd April 2020

DOI: 10.1039/d0py00336k

rsc.li/polymers

1. Introduction

Sensors provide a communication interface between humans and the surrounding world. To perceive external signals, during the long period of evolution, the human body has formed five sets of sensors, that is nose, tongue, eyes, ears, and skin.[1] Inspired by nature, chemists have also been working on developing synthetic chemical sensors to detect various analytes due to their significance in biomedical analysis and environmental protection.[2] Chemical sensors with fluorescence as the output signal, commonly called fluorescent

[a]*School of Materials Science and Engineering, Nanjing Institute of Technology, Nanjing, 211167, P. R. China*
[b]*Jiangsu Key Laboratory of Advanced Structural Materials and Application Technology, Nanjing, 211167, P. R. China*
[c]*Institute of Physical Science and Information Technology, Anhui University, Hefei 230601, China*
[d]*Institute of Pharmaceutical Sciences, Department of Chemistry and Applied Biosciences, ETH Zurich, 8093 Zurich, Switzerland.*
E-mail: yinyin.bao@pharma.ethz.ch

Taisheng Wang

Taisheng Wang received a BS degree in polymer materials and engineering from the Hefei University of Technology (2011) and a PhD in chemistry from the University of Science and Technology of China (2017). He is currently a lecturer of the Department of Polymer and Composite Engineering at Nanjing Institute of Technology. His scientific interests mainly concern the preparation of chemically and mechanically responsive polymeric materials, and synthesis and characterization of self-strengthening polymers.

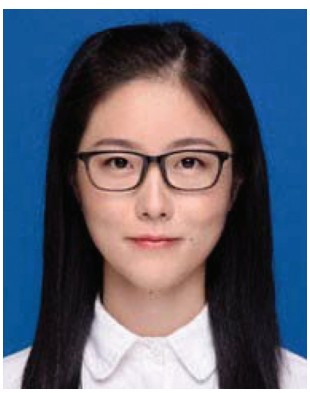

Na Zhang

Na Zhang received a BS degree in polymer materials and engineering from the Hefei University of Technology (2013) and a PhD in chemistry from the University of Science and Technology of China (2018). She is currently a lecturer of the Department of Polymer and Composite Engineering at Nanjing Institute of Technology. Her scientific interests mainly focus on the design and synthesis of two-dimensional materials and the preparation of chemically and mechanically responsive polymeric materials.

chemosensors, have exhibited great advantage compared to traditional analytical methods, such as mass spectrometry,[3] Raman spectroscopy[4] and ion mobility spectroscopy.[5] This is because fluorescence signals can enable high sensitivity and selectivity, fast measurement, low cost, *in situ* analysis, and sometimes even "naked eye" detection. Fluorescent chemosensors are generally designed based on one system which consists of two key components: a receptor and a fluorophore. The receptor can selectively interact with a specific analyte in a certain way, usually through coordination, ionic interaction, hydrogen bonding, or chemical reaction, and thereafter the fluorophore can change its photophysical properties when the interactions between the receptor and analyte occur.[6] In particular, a certain spacer connecting the two components can also be introduced to optimize the sensing performance in some cases.[7]

Fluorescence sensing usually utilizes one of the following characters: mostly the fluorescence intensity change ("turn-on" or "turn-off") and spectral shift (emission color change), as well as the fluorescence life time variation and polarization change, to a lesser extent.[8] These changes may be triggered by interactions between sensors and analytes of interest. In general, the performance of a fluorescent chemosensor is usually determined by its selectivity and sensitivity. Other characteristics including the response time, recovery time, reversibility, overall lifetime, and cost, are also considered for real applications. In addition, like any other analytical tools, the ease of use, high accuracy, and acceptable reproducibility of the results are also expected from the sensors.[9] Among various fluorescent chemosensors from different materials, π-conjugated polymer (CP)-based sensors have attracted much attention as they can be used to detect a variety of environmental pollutants and bioactive compounds, owing to their amplified detection sensitivity. These conjugated polymers are referred to as amplifying fluorescent polymers, typically with distinctly high sensitivity for fluorescence sensing, benefiting from their ability to transport electronic excited states. According to the theory of Swager and coworkers, who first developed CP-based chemosensors,[10a] excitons in excited states can rapidly migrate throughout the conjugated polymer chain or even diffuse within the bulk solid state. This is due to both space dipolar couplings and strong mixing of electronic states; thus the polymer backbone can be viewed as a molecular wire. When CPs are constructed as a detection system, once an analyte appears and interacts with the receptor moiety of the polymer sensor, the excitation electron/energy transfer from the CP to the analyte will occur immediately along the whole polymer backbone. As a consequence, a greatly amplified signal can be achieved, resulting in enhanced sensitivity, a unique benefit that conventional molecular sensors do not possess. Moreover, different from fluorescent chemosensors based on small molecules, the CP-based sensors also display excellent film-forming properties and high flexibility for chemical design and structure modification.[10b–e]

Since the report of the first example by Swager and coworkers in the 90s,[10f] the CP-based sensing strategy has achieved more than two decades of progress, with an explosion of the research in this field observed in the last ten years.[10g,h] A number of CP-based fluorescent chemosensors have been developed with various polymer backbones and receptor moieties, and they have exhibited profound potential in biosensing and environmental analysis, including metal ion/anion detection, biomolecule sensing, bioimaging, explosive detection, *etc*.[11] A series of comprehensive review papers have also been published on this topic;[11a,b,f,g] however, to our knowledge, there is still no such review that exclusively focuses on the nitrogen receptor moiety of the CP sensors, especially for the ones based on aromatic N-heterocycles. The conjugated polymers with aromatic N-heterocyclic moieties indeed played

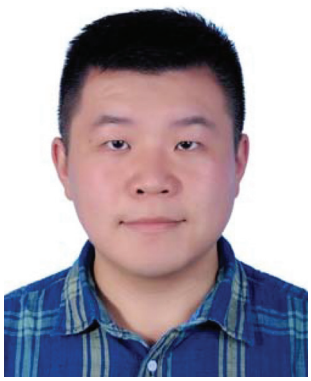

Wei Bai

Dr Wei Bai has been a Professor at the Institute of Physical Science and Information Technology of Anhui University since 2018. He received his PhD (2014) from the Department of Chemistry of Louisiana State University – Baton Rouge and worked as a Postdoctoral Research Associate at the University of Massachusetts and the University of Tennessee for three years before joining the Anhui University. His area of interest focuses on the synthesis of novel polymeric and supramolecular materials, especially organic 2D polymers and functional fluorescent molecules.

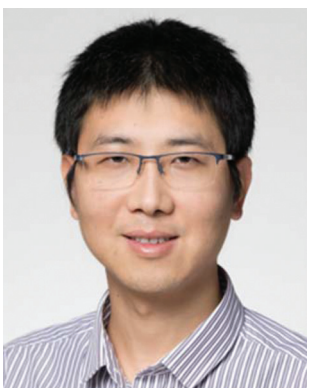

Yinyin Bao

Yinyin Bao is a group leader in the Institute of Pharmaceutical Science at ETH Zürich. He received his PhD degree in Polymer Chemistry from the University of Science and Technology of China (2012). After completing his postdoctoral research at KU Leuven, he became a Marie Curie IntraEuropean Fellow in CNRS & Univ. Paris Sud. In 2016, he joined ETH Zürich, and he was promoted to a Senior Scientist position in late 2018. His research interest remains the application of synthetic molecules and polymers in the biomedical area, such as fluorescence sensing and imaging, drug delivery, 3D printed medical devices, etc.

a pivotal role during the development process of CP sensors,[12] with the first example employing a 2,2′-bipyridyl group reported in 1997 by Wasielewski and coworkers.[12c] On the occasion of the 100th anniversary of polymer chemistry, we would like to take this opportunity to give a summary of the two decades of evolvement. In parallel, as a witness and also a contributor to the progress in such an exciting research area, we will provide a perspective on the possible future research directions. This review focuses on the CP-based fluorescent chemosensors with aromatic N-heterocyclic moieties, and the polymers are classified according to the different N-ligands employed. Due to the characteristics of these heterocycles, metal ions are the main analytes of interest, with also protons, anions and other biomolecules as the targets of detection, to a lesser extent.

2. Aromatic N-heterocyclic receptor moieties

As one of the two key components of CP sensors, the receptor moiety is crucial for achieving optimal detection performance. Many different types of interactions between analytes and receptors have been utilized in the previous reports, such as Lewis acid and base interactions,[13] collision quenching,[14] formation/cleavage of chemical bonds,[15,16] *etc*. Among these detection mechanisms, the Lewis acid and base interaction is the most frequently used strategy, owing to the rapid response. The receptors used in this situation are always the electron donating units containing nitrogen, sulphur or phosphorus atoms. In these polymers, the aromatic N-heterocyclic receptors, especially for pyridine, imidazole and their derivatives, occupy a prominent position, and have been successfully introduced into either the main chains or side groups of the polymers. When the interactions between these receptor moieties of the CP sensors and different analytes occur, the fluorescence of these polymers can exhibit significant changes such as quenching, emission red or blue shifts, and fluorescence enhancement, to a lesser extent. This is a result of photoinduced electron transfer (PET), the enhancement/decrement of the conjugation or the electron transfer between the polymer and analytes (*e.g.*, FRET). In this review, we summarize the related works on fluorescent CP chemosensors according to the different types of aromatic N-receptors, including pyridine-based (mono-pyridine, 2,2′-bipyridine, and terpyridine), imidazole-based (mono-imidazole and 2,2′-biimidazole) and fused heterocycles (quinoline, 1,10-phenanthroline and their derivatives), as shown in Fig. 1. Due to the highly rigid backbone and strong hydrophobicity of conjugated polymers, the fluorescence sensing is usually conducted in organic solvents; thus the description in the review is always considered as not in aqueous solutions, if not mentioned specifically. In general, the fluorescence quantum yield of these conjugated polymers is usually quite high; thus concrete values will not be given for each case in the later descriptions.

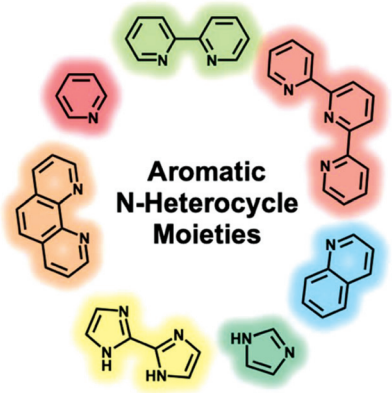

Fig. 1 The aromatic N-heterocyclic moieties that were introduced to conjugated polymer-based fluorescent sensors summarized in this review.

3. Pyridine-based CP chemosensors

3.1. 2,2′-Bipyridine-based CP chemosensors

Since the discovery of bipyridine groups in the late 19th century, they have been widely reported for constructing various functional polymers. Among the symmetrical isomers of bipyridine (2,2′, 3,3′, and 4,4′), the 2,2′-bipyridine ligand has been extensively applied as a metal coordinating ligand due to its strong redox stability and easy functionalization.[17] It was described as "the most widely used ligand" and this status has not changed until now, which can be confirmed by the frequent use of 2,2′-bipyridine in atom transfer radical polymerization (ATRP).[18] The most common coordination mode of 2,2′-bipyridine is as a chelating bidentate ligand in which both nitrogen atoms are bonded to the same metal centre.[19] In a transoid-like conformation, there is a 20° dihedral angle between two pyridine planes. When incorporated into the backbone of a CP, this polymer is not completely conjugated. However, when coordinated with a metal ion, the coordination interaction would cause the transformation of the transoid-like conformation into a planar one which enhances the conjugation degree of the polymer.

The first example of a 2,2′-bipyridine based CP sensor (**CP-1**) was reported by Wasielewski and coworkers, and it is also one of the earliest CP-based fluorescent sensors.[12] **CP-1** was designed to be partially conjugated in its metal free state. A number of metal ions could induce ionochromic effects. Upon incorporation of metal ions, the polymer underwent conformational changes, therefore converting to a nearly fully conjugated form along with the variation of the optical properties. The metal ion size, coordinating ability and redox properties are all responsible for the fluorescence response. Treating the polymer–metal ion complex with competitive ligands could convert it to its original metal free polymer state. Similar work has also been reported by Ciou *et al.*[20] Moreover, Wang and coworkers found that tuning the electron density of the backbone through incorporating a fluorene structural unit (**CP-2**) could vastly improve the detection selectivity.[21] By tailoring the

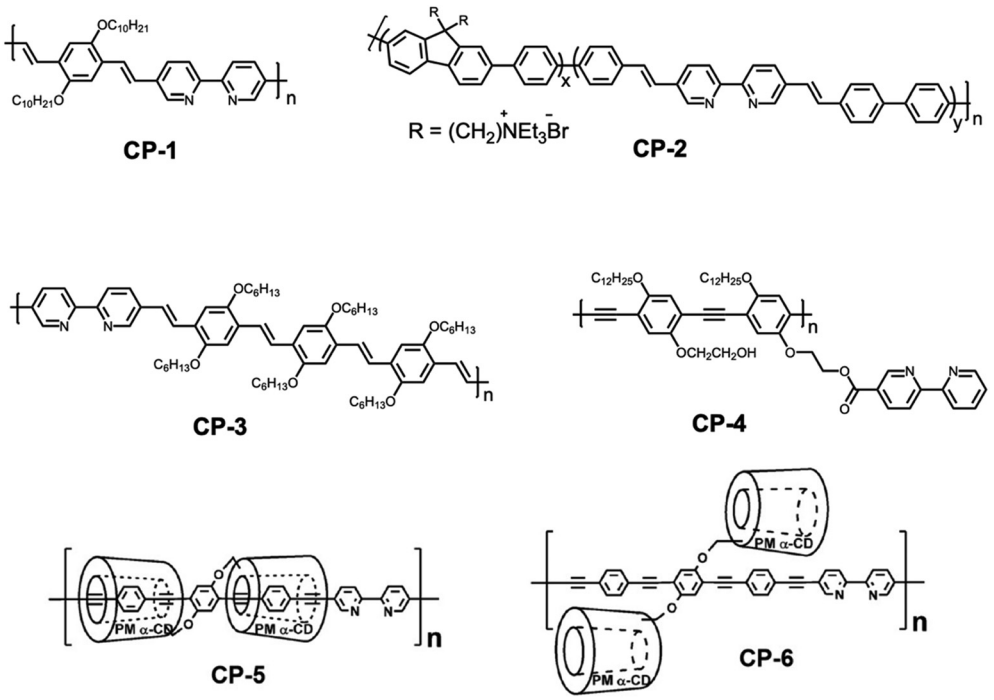

Fig. 2 The representative chemical structures of 2,2′-bipyridine-contained CP chemosensors.

fluorene unit fraction of the polymer backbone, the sensing selectivity and sensitivity of **CP-2** to Cu^{2+} could be efficiently manipulated. Under optimal conditions, the Stern–Volmer constant values (K_{SV}) could be as high as 1.44×10^7 M^{-1}. In this work, cationic side chains were introduced to the system; thus the resulting conjugated polyelectrolytes could realize the selective detection of Cu^{2+} in aqueous solutions.

Cu^{2+} could be reduced to Cu^{+} in the presence of nitric oxide. This change in the valence was reflected in turn on the emission of the Cu^{2+}–polymer complex. Based on this mechanism, Lippard *et al.* constructed a bipyridine containing poly(*p*-phenylene vinylene) derivative (**CP-3**) for the fluorescence detection of nitric oxide (NO) with a "turn on" mode.[22] Cu^{2+} was able to efficiently quench the fluorescence of **CP-11** by forming a coordinative crosslinking metal–polymer network.[23] However, the bubbling of NO into the **CP-3**–Cu^{2+} solution reduced it to the **CP-3**–Cu^{+} complex, accompanied by a prominent increase in the fluorescence intensity (Fig. 3). The detection process is free from the interference of other biological reactive nitrogen species.

With regard to most of the conjugated polymers with 2,2′-bipyridine moieties on the main chain, the strong coordination ability with a large array of metal ions resulted in unsatisfactory selectivity. Surprisingly, by attaching the ligand as pendant groups, the selectivity could be more finely tuned, while still retaining the advantages of the CP backbone. For instance, the fluorescence of a poly(*p*-phenylene ethynylene) derivative with pendant 2,2′-bipyridine groups (**CP-4**) could be selectively quenched with Hg^{2+}, with negligible influence of other metal ions.[24] Note that the detection limit was found to

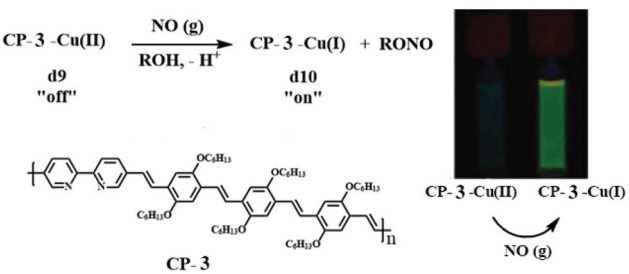

Fig. 3 The sensing mechanism of **CP-3** for NO. Inset shows the fluorescence images of **CP-3**–Cu(II) after bubbling the NO gas. Reproduced with permission from ref. 22. Copyright 2005, American Chemical Society.

be 8.0 nM, which is relatively lower than those of other similar systems (Fig. 2).

Despite the excellent performance of the 2,2′-bipyridine-based CP sensor in the solution state, it is more challenging to use them in the solid state as films, due to the self-quenching of the emission caused by strong intermolecular π–π interactions. Terao *et al.* proposed an interesting method to tackle this issue.[25] They synthesized a α-cyclodextrin (α-CD) insulated CP containing 2,2′-bipyridine receptor (**CP-5**). The α-CD group with large steric hindrance restricted the close packing of polymer chains. As a result, even in the solid state, the polymer exhibited strong emission, and the emission spectra of the films are comparable to those of dilute solutions. The complexation ability of **CP-5** was sustained, leading to a fluorescence change in response to metal ions (Fig. 4). The

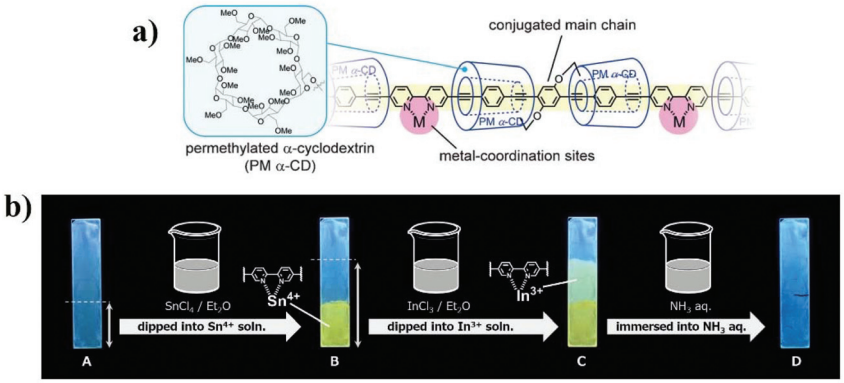

Fig. 4 The chemical structures of **CP-5** (a); change in the emission color of the **CP-5** film with exposure to metal ions (b). Photographic images were taken under UV irradiation at 365 nm. Double-headed arrows indicate the dipped regions of the films. Reproduced with permission from ref. 25. Copyright 2016, John Wiley and Sons.

luminescence color changes induced by different metal ions were easily erased through removal of the coordinated metals by immersion in an aqueous NH_3 solution. The emission properties of **CP-6** are quite different from those of **CP-5**. With the linked α-CD restricted rotation of the aryl rings in phenyleneethynylene, the Stokes shift of **CP-5** was significantly smaller than that of **CP-6** in dilute solution. Meanwhile, a 100 nm red-shift of the emission maxima was observed for **CP-6** in the solid state.

3.2. Mono-pyridine-based CP chemosensors

Despite the frequent use of bipyridine in fluorescence sensing, the single pyridine group, as a six-membered heterocyclic moiety, is also a potential receptor unit for constructing a chemosensor.[26] Pyridine has lone pair electrons on nitrogen, which endow it with weak alkalinity and strong coordination ability. For example, Uwe H. F. Bunz and coworkers synthesized a pyridine-containing poly(aryleneethynylene) (**CP-7**).[27] The presence of the pyridine unit afforded **CP-7** multiple fluorescence responsive behaviors including acidochromicity, solvatochromicity and metallochromicity (Fig. 6). Due to the varied polarity, the emission color of **CP-7** covers from blue to green and yellow in various organic solvents, as a result of the aggregation-induced planarization of the backbone. On protonation, the pyridine ring becomes a stronger electron accepting unit, and thus the donor–acceptor character is much more significant. The red-shift in fluorescence upon addition of TFA was observed as a consequence.

Due to the limited water solubility of the CP chemosensors because of extended π-conjugation, it is challenging for these sensors to be used in aqueous environments. In order to overcome this challenge, water soluble branched oligoethylene glycols (swallowtail) were introduced to the polymer side groups, and a series of CPs with relatively high fluorescence quantum yields were synthesized.[28] Take **CP-8** for example; it emitted in a range from 450 to 500 nm in water with a fluorescence quantum yield of 0.18. Upon protonation, a red-shift and emission intensity decrease could be observed, which is a consequence of enhanced internal charge transfer. Transition metal ions such as Cu^{2+}, Hg^{2+}, and Fe^{3+} were strong fluorescence quenchers while the quenching effect was weaker for the other metal ions such as Al^{3+}, Co^{2+}, and Zn^{2+} (Fig. 5).

Recently, Bhattacharya and coworkers showed that π-conjugated *p*-phenylenevinylene oligomers with a pyridine unit as the end group can selectively detect Hg^{2+}.[29] Addition of Hg^{2+} caused a distinct change in the color of **CP-9** solutions from colorless to yellow accompanied by the transformation of the fluorescence from blue to intense yellow. Owing to the interaction of Hg^{2+} with the nitrogen-containing pyridine moiety, the polymers can form two-coordination complexes. Such complexes facilitate the intramolecular charge transfer process resulting in red-shifts in both absorption and emission bands. Although the visual response was more pronounced for oligomer **CP-10** with a higher conjugation length, the selectivity and sensitivity toward Hg^{2+} was compromised due to its higher degree of self-aggregation, lower basicity of pyridyl nitrogen and restricted molecular motion (Fig. 7).

Li and coworkers employed di(2-picolyl)amine moieties as the receptor group to construct a functional fluorene/carbazole copolymer sensor (**CP-11**).[30] The three lone pairs on the receptor unit could synergistically bind with Cu^{2+} tightly, leading to complete quenching of the fluorescence of the polymer. Alkali and alkaline earth metal ions have no influence on the fluorescence of the polymer due to their poor coordination ability with the receptor units. Other transition metal ions such as Ag^{+}, Zn^{2+} and Hg^{2+} could also quench the fluorescence, but to a lesser extent. This CP sensor showed great advantages over small molecules bearing the same receptor unit, such as much higher sensitivity and better selectivity, indicating that the sensing properties of molecular sensors could be optimized by chemical derivatization by extending π-conjugation. In addition, the quenched peak of the complexes can be gradually recovered when CN^{-} is added into the solutions. This is because CN^{-} could form very stable $[Cu(CN)_x]^{n-}$ complexes with copper ions, and thus the ligand can be displaced. This work demonstrates that the

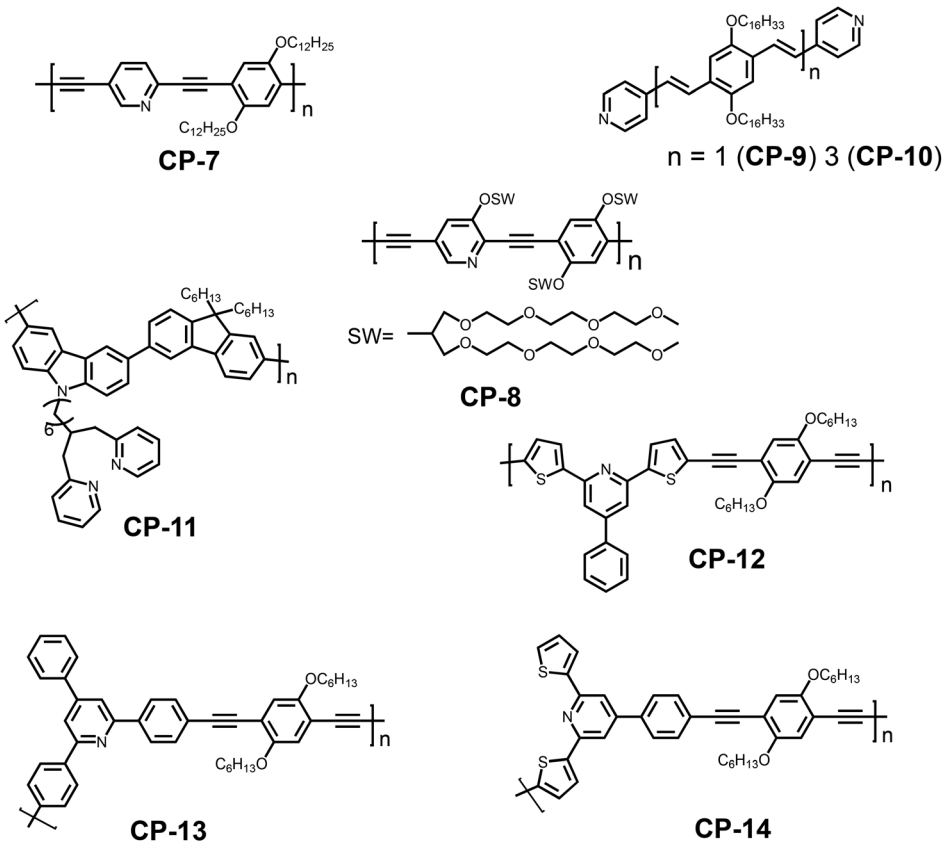

Fig. 5 Chemical structures of the representative fluorescent chemosensors based on the mono-pyridine group containing conjugated polymers/oligomers.

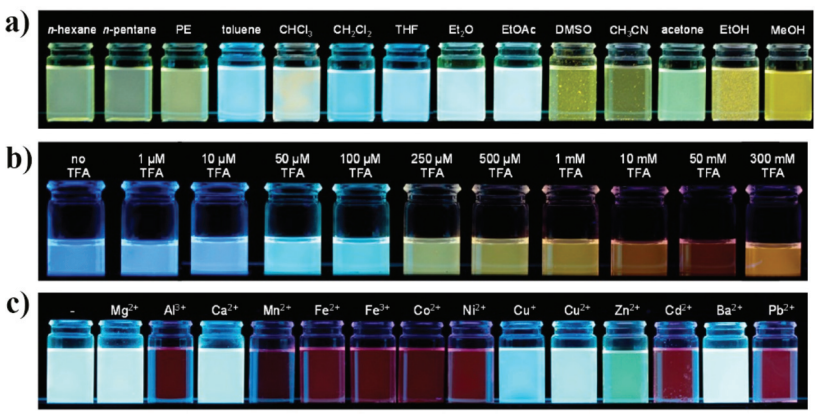

Fig. 6 Photographs of **CP-7** in different solvents (a), with increasing content of trifluoroacetic acid (TFA) (b) and different metal ions (c) under a hand-held black light with illumination at 365 nm. Reproduced with permission from ref. 27. Copyright 2014, American Chemical Society.

polymer–Cu^{2+} complex could also be used to detect CN^- based on the replacement strategy.

In 2011, Bai and coworkers reported a series of fluorescent CPs containing 2,6-bis(2-thienyl)pyridine moieties (TPP). Since the sulfur atom is considered as a "soft" donor atom in a chelating agent, it generally increases the sensor's affinity for "soft" metals. The resulting **CP-12** showed excellent selectivity for Pd^{2+}.[31] As a result of the Pd^{2+} ion induced intra-chain linkage, an obvious color change from yellow green to brown was observed, while the fluorescence intensity at 472 nm dramatically decreased. Although **CP-12** was also responsive to Pt^{4+}, the quenching was much weaker than that induced by Pd^{2+}. Thus, the interference from Pt^{4+} could be prevented basically, and it was superior to the Pd^{2+} sensor

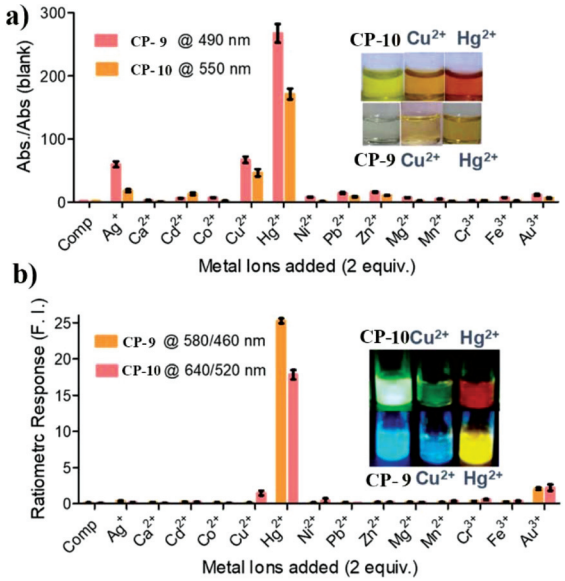

Fig. 7 Changes in (a) the absorbance and (b) fluorescence of **CP-9** and **CP-10** (10 μM) with different metal ions (2 equiv.) in THF. Insets showing the resulting solutions in day-light and under 365 nm UV-light, respectively. Reproduced with permission from ref. 29. Copyright 2019, American Chemical Society.

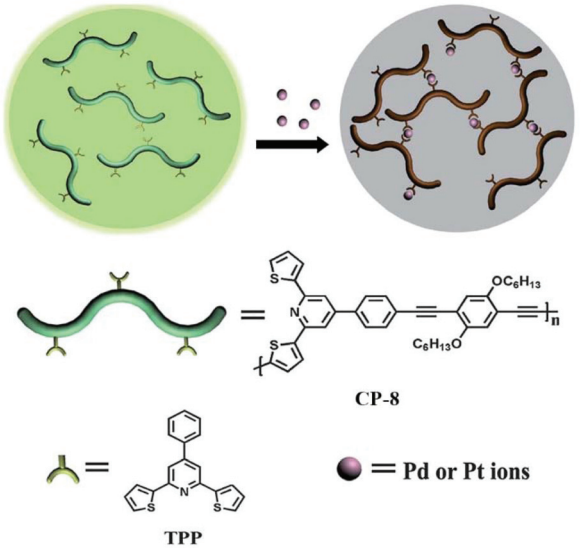

Fig. 8 Schematic illustration of the sensing mechanism of **CP-14**. Reproduced with permission from ref. 34. Copyright 2012, The Royal Society of Chemistry.

based on the *meta*-acetenyl substituted pyridine moiety developed by Wang *et al.*[32] As expected, when the thiophene groups on the 2,6-dithienyl-4-phenylpyridine units were replaced by benzene groups, affording **CP-13**, no fluorescence change was observed after the metal ions were added to the polymer solutions.[33] This could be attributed to the steric hindrance effect of two benzene rings at the two *ortho* positions of pyridine. If the acetylene group with smaller size replaces benzene groups attached to the two *ortho* positions of pyridine, it becomes an efficient receptor for metal ion coordination again. The steric hindrance of the coordination units (TPP) embedded in the polymer chain is crucial to the selectivity of the polymer for Pd^{2+} and Pt^{4+}.[34] For less steric hindrance polymer **CP-14**, the detection limits based on the UV-Vis absorption change for Pd^{2+} and Pt^{4+} are both less than 1×10^{-6} M, and the fluorescence intensity also significantly decreased on the addition of Pd^{2+} and Pt^{4+} with almost the same quenching degree (Fig. 8), while for the polymer **CP-12**, owing to the more restricted thiophene group in the TPP units, the quenching degree induced by Pd^{2+} is approximately three times larger than that caused by Pt^{4+}. This demonstrated the feasibility of varying the polymer structures to match the molecular spatial dimensions for controlling the metal ion selectivity.

To our understanding, due to the versatile coordination ability with various metal ions, the selectivity of the mono-pyridine containing CP sensors is usually not outstanding without derivatization. However, when other supportive co-ligands/groups are introduced, the sensing performance could be greatly improved.

3.3. Terpyridine-based CP chemosensors

Besides bipyridine and mono-pyridine in the pyridine family, terpyridines and their derivatives have also evoked extensive research interest in the area of coordination chemistry and materials science.[35] The strong binding affinity towards a variety of metal ions has brought about diverse supramolecular architectures and a wide range of potential applications including photovoltaic conversion,[36] light emitting devices,[37] DNA binding,[38] anti-tumor active agents and catalytic applications.[39] On top of that, the dendritic terpyridine ligands can form polymetallic species which then can be utilized as fluorescent sensors or to construct supramolecular architectures. Terpyridine is a tridentate pincer ligand which can tightly coordinate with various metal ions in a planar geometry. Based on the number of coordination units used, terpyridine has two possible coordination patterns: mono-pincer complexes and bis-pincer complexes.[40] To avoid the electrostatic repulsion of the lone pair electrons on nitrogen atoms, the 2-pyridine adopts a *trans* geometry before coordinating with the metal ion. On chelation, a *cis* geometry is formed, and the pyridines take a perfect planar conformation consequently, which is similar to the bipyridine groups. This character enables terpyridine to be a potential recognition unit for sensing applications. In particular, CP sensors with terpyridine units as recognition sites have gained considerable attention recently for their high detection sensitivities.

The pioneering work regarding the terpyridine-based CP sensors was reported by Shirai *et al.* in 1998.[41] The synthesized *ortho*-terpyridine substituted poly(*p*-phenylenevinylene) (**CP-15**) exhibited its sensing ability to various transition metal ions, while the control polymer, which lacked the terpyridine segments as recognition sites, showed no change in the photo-

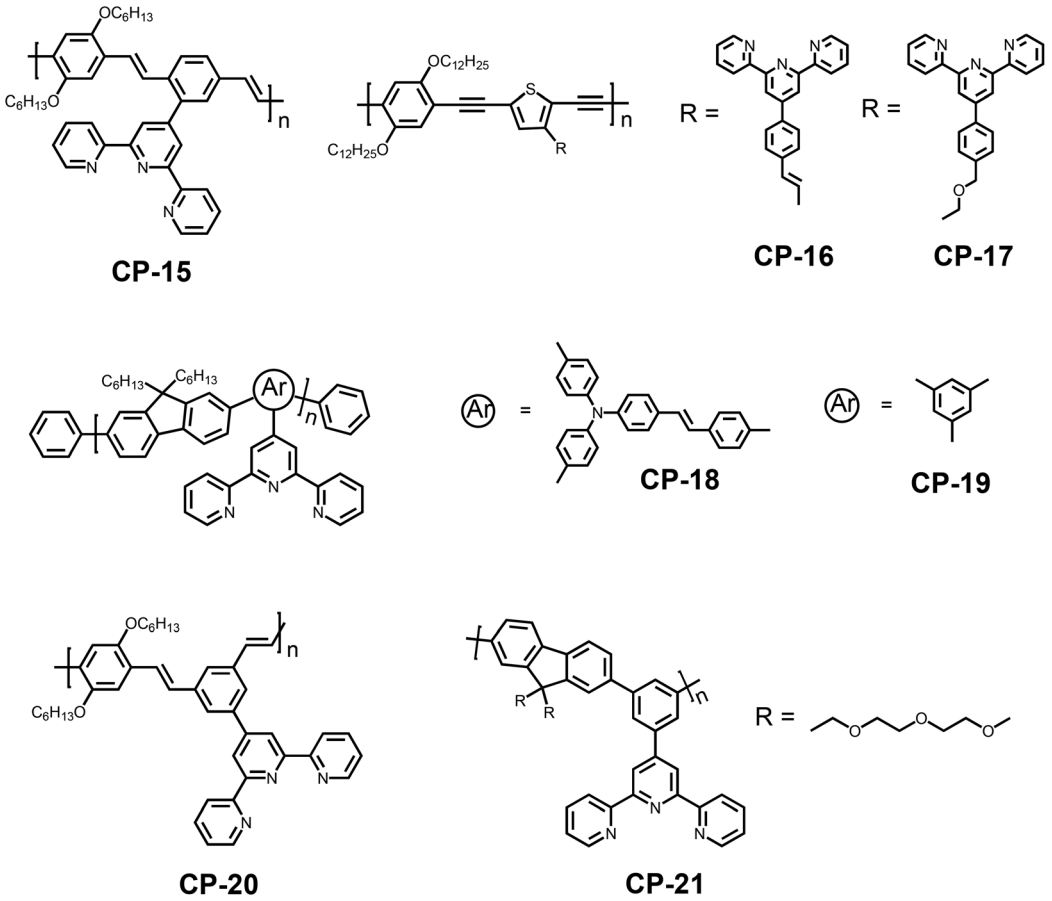

Fig. 9 Chemical structures of the representative terpyridine-based CP chemosensors.

physical properties. In the presence of metal ions such as Fe^{2+}, Fe^{3+}, Ni^{2+} and Cu^{2+}, complete fluorescence quenching was observed, due to the energy transfer between the metal complexes and the polymer backbone. However, Zn^{2+} ions brought about a red shift of the emission band, which occurred due to an intra-ligand charge transfer state, originating from the conjugated main chains to the zinc-terpyridine complexes. A systematic study concerning the Zn^{2+} ion induced ionochromic mechanism of a terpyridine-based CP has been reported.[42] Regarding the CP sensors incorporating a terpyridine moiety, generally, complete conjugation between the recognition unit and backbone is not required for emission quenching, although the fully conjugated ones show higher quenching efficiency for Ni^{2+} (**CP-16** and **CP-17**).[43]

The chemical structure of the polymer backbone and recognition unit, as well as the substitution position of the terpyridine group on the main chain have prominent influence on the detection sensitivity or selectivity of the CP sensors (Fig. 9).[44] For example, the polymer with a higher degree of conjugation (**CP-18**) showed much higher sensitivity to Cu^{2+} compared with **CP-19**, which has a lower conjugation level (the K_{SV} value is 2.3×10^5 M^{-1} for **CP-18** and 1.05×10^5 M^{-1} for **CP-19**). This is a result of enhanced intermolecular interactions between the receptor–Cu^{2+} complex and the backbone.[44a] Accordingly, the complex was used to detect CN^- ions by the displacement mechanism, and it also showed a similar difference in the sensitivity. The influence of the substitution position of the recognition unit on the detection selectivity was also observed.[44b] Greater fluorescence quenching in the presence of Cu^{2+} ions was found in the solution of *meta*-phenylene-containing poly(phenylenevinylene) with a pendant terdentate terpyridine ligand (**CP-20**) (with the quenching level in the order of $Cu^{2+} > Co^{2+} > Ni^{2+} > Hg^{2+} > Zn^{2+} > Cd^{2+}$), while Cr^{3+}, Fe^{3+}, and Mn^{2+} ions could not quench the fluorescence. The results are in contrast to those of its isomeric polymer **CP-15**, whose fluorescence in solution has been reported to be completely quenched by Fe^{3+}, Ni^{2+}, Cu^{2+}, Cr^{3+}, Mn^{2+} and Co^{2+}. Regarding the complex **CP-20**/M^{2+}, the resonance interaction from the terpyridine center is only transmitted up to the *meta*-phenylene bridge. The molecular design of **CP-20** limits the resonance interaction between the terpyridine and polymer backbone, thereby attenuating the metal ion-induced fluorescence quenching to allow the observed selectivity (Fig. 10). This structural design strategy has judiciously been applied to poly(metaphenylene-*alt*-fluorene) with *meta*-substituted terpyridine as a Cu^{2+} sensor (**CP-21**), to enhance the fluorescence detection selectivity with a K_{SV} of about 4.1×10^5 M^{-1} (Fig. 11).[44c]

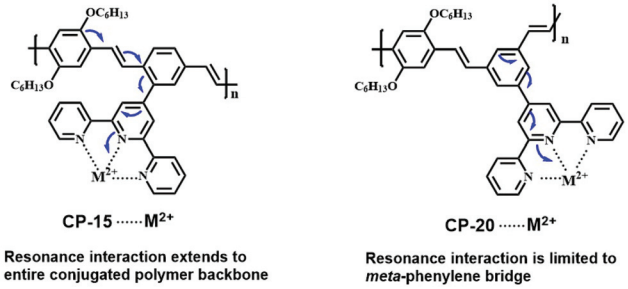

Fig. 10 Resonance interactions for **CP-15**–M^{2+} and **CP-20**–M^{2+} complexes. Reproduced with permission from ref. 44*b*. Copyright 2009, Elsevier.

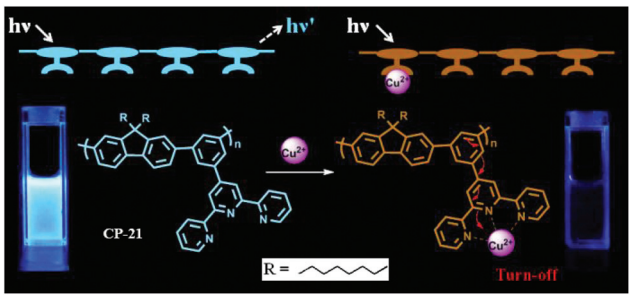

Fig. 11 Sensing mechanism of **CP-21** for Cu^{2+}. Reproduced with permission from ref. 44*c*. Copyright 2018, Elsevier.

4. Imidazole-based CP chemosensors

4.1. Mono-imidazole-based CP chemosensors

The imidazole ring exists extensively in nature and plays an important role in many bioactive structures within the human body, such as histidine and ergamine.[45] Most uses of the imidazole ring as a bioagent revolve around its ability to bond to metal ions as a ligand, as well as the formation of hydrogen bonds with molecular drugs and proteins.[46] The NH proton of the imidazole exhibits weak acidity, which can be tuned by changing the electronic properties of the imidazole substituents. On the other hand, the donor pyridine-like nitrogen atom shows weak alkalinity. Due to its amphoteric nature, the imidazole ring and its derivatives can function as either a selective anion or a cation receptor.

In 2003, Leclerc and coworkers first reported an imidazole substituted conjugated polythiophene (**CP-22**) for naked eye iodide-specific detection.[47] The process is free from the disturbance of a wide range of other anions including F^-, Br^- and Cl^-. The exact sensing mechanism is that the iodide anions induced planarization and aggregation of the polymer, leading to the enhancement of the polymer conjugation length. Since then, a series of studies related to imidazole-based CP sensors have been vigorously performed.[48] For example, in order to detect metal ions in aqueous media, the polyfluorene functionalized in the side chain with imidazole moieties (**CP-23**) was covalently attached to a polymethacrylic acid matrix.[48*b*] Based on a microemulsion polymerization procedure, fluorescent CP microspheres were prepared. The carboxyl groups in this structure facilitate the dispersion of the microspheres, and also favor the penetration of water into the structure. The prepared microspheres were highly sensitive and selective to Cu^{2+} compared with other divalent cations. Compared with the bulk polymer, this polymer microsphere sensor showed unique advantages such as an improved selectivity, stronger stability and a faster regeneration after coordination with the metal ion for subsequent reuse (Fig. 12).

The interaction between Cu^{2+} and imidazole is relatively weak. Thus, with the addition of the strong complexing unit, Cu^{2+} can be deprived from the Cu^{2+}–polymer complex, leading to a recovery of the fluorescence. Based on this replacement strategy, an imidazole-functionalized polyfluorene (**CP-24**) was used as a selective chemosensor for Cu^{2+} and further for cyanide.[49] Since the imidazole groups could enable efficient energy transfer from the conjugated backbone to Cu^{2+}, the fluorescence of this polymer could be completely quenched by Cu^{2+} at concentrations as low as 0.2 ppm. Owing to the fact that CN^- has strong binding affinity with Cu^{2+}, when CN^- was added to the solution of the Cu^{2+}–polymer complex, the coordination between the Cu^{2+} and imidazole groups was destroyed, accompanied by the recovery of the blue fluorescence. This indirect strategy to probe CN^- could be used to design new anion sensors. Tang *et al.* replaced the main chain into polyacetylene to synthesize an imidazole-functionalized polymer (**CP-25**).[50] This sensor also showed high detection sensitivity toward Cu^{2+}, but the detection selectivity is superior to those of other CPs containing imidazole moieties with little influence from other transition metal ions, indicating that the sensing properties could be adjusted by tailoring the backbone structure. In the solid state, the polymer was still emissive, and thus could be used in a film form. Similarly, the resulting Cu^{2+}–polymer complexes were available for sensing CN^- and α-amino acids based on a replacement mechanism. The completely quenched fluorescence of **CP-25** by Cu^{2+} was turned on after the addition of CN^- at concentrations as low as 7.0×10^{-5} M. Other anions caused nearly no disturbance to the selective sensing of CN^-, except for a little influence from HPO_4^{2-} and PO_4^{3-} (Fig. 13).

Zhu *et al.* synthesized a cationic **CP-26**, containing an imidazole moiety and water-soluble quaternary ammonium salt groups, which was used for nitric oxide detection in aqueous solutions.[51] In the presence of Cu^{2+} ions, the fluorescence of the polymer was efficiently quenched through a photo-induced electron transfer (PET) process. Upon the addition of nitric oxide, paramagnetic Cu^{2+} was reduced to diamagnetic Cu^+, inhibiting the PET process; therefore, the fluorescence of the polymer was recovered. Different from the replacement mechanism that is mentioned above, the Cu^+ ions still bind to the imidazole receptors instead of being snatched by another ligand during the sensing process.

Recently, Patra *et al.* synthesized a highly emissive conjugated polymer containing fused imidazole moieties on the

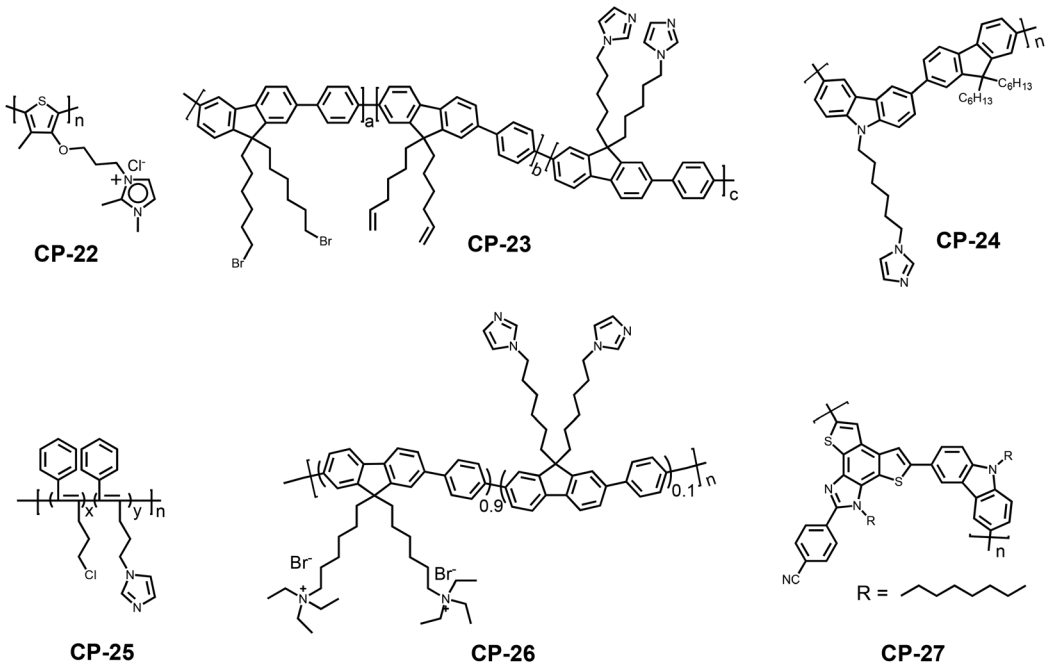

Fig. 12 Chemical structures of the representative mono-imidazole-based CP sensors.

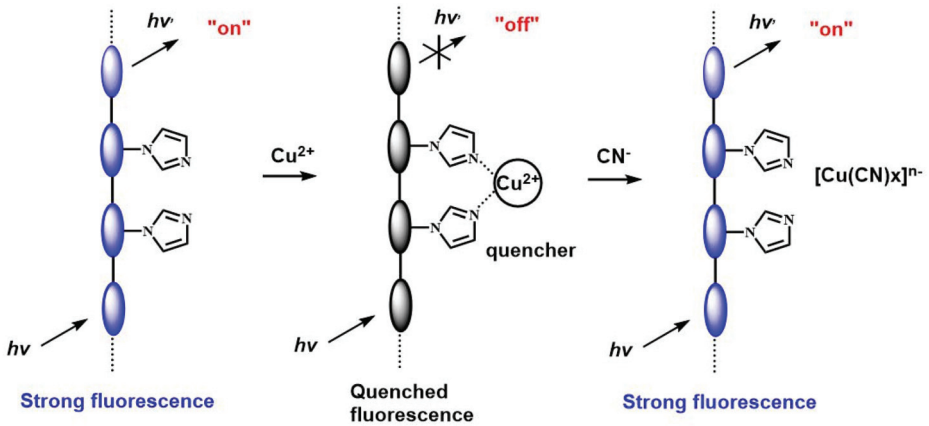

Fig. 13 Schematic representation of Cu^{2+} and CN^- sensors based on the fluorescence "turn-off" and "turn-on" of the polyacetylene. Reproduced with permission from ref. 50. Copyright 2008, The Royal Society of Chemistry.

main chain (**CP-27**) through Suzuki coupling polymerization.[52] The nitrogen and sulphur donor atoms of the fused heterocycle can serve as efficient coordinating sites for Hg^{2+} ions. Upon treatment with Hg^{2+}, a prominent turn-off fluorescence response was observed with the detection limit found to be in a range of 40–50 ppb (Fig. 14). Interestingly, all the other competing metal ions do not interfere with the detection process. The polymer–Hg^{2+} complex is reversible essentially, and can further serve as a sensor for S^{2-}, due to the displacement.

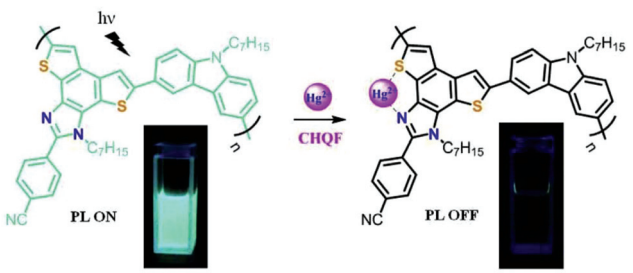

Fig. 14 Proposed sensing mechanism for **CP-27**. Reproduced with permission from ref. 52. Copyright 2019, Elsevier.

4.2. 2,2-Biimidazole-based CP chemosensors

2,2′-Biimidazole, the dimeric analogue of imidazole, is one of the most important derivatives of imidazole, and plays a par-

ticular role in crystal engineering because of its excellent coordination ability and diverse coordination modes.[53] Despite 2,2′-biimidazole being first obtained by Debus in 1858,[54] the chemistry of this biheterocyclic compound had received little attention due to the fact that the synthesis of the bicyclic structure is very laborious. Furthermore, the extremely poor solubility of 2,2′-biimidazole in organic solvents has restrained its direct functionalization.[55] However, the 2,2′-biimidazole unit indeed possesses great potential in various fields such as materials science[56] or pharmacology,[57] benefiting from its structural features, including the multi-nitrogen atom and π-conjugation. Hence, the functionalization of 2,2′-biimidazole is of great importance in view of full tapping potential for its application. Triggered by this motivation, various strategies have been developed to functionalize 2,2′-biimidazole easily under mild conditions.[58] In particular, the unique structure associated with 2,2′-biimidazole can guarantee it as an ideal N,N-bidentate ligand for constructing novel coordination complexes, with potential for use in antitumour drugs, bioinorganic chemistry, catalysis, organic light-emitting diodes, chemosensors and supermolecular frameworks.[59] In 2003, 2,2′-biimidazole-based homopolymers were prepared by dehalogenative polycondensation by Yamamoto's group.[60] Later on, MacLean *et al.* successfully prepared CPs with the 2,2′-biimidazole moiety *via* electrochemical polymerization.[61] Different from 2,2′-bipyridine, 2,2′-biimidazole has a large M–N (metal–nitrogen) bond length of 4.2 Å, instead of 2.51 Å, which might endow CP sensors with distinguishing sensing properties. However, the 2,2′-biimidazole moiety did not attract much attention from researchers in the field of CP sensors in the first decade of the 2000s. Until 2011, we designed and synthesized a series of novel 2,2′-biimidazole-incoporated conjugated polymers, which opened new perspectives of efficient fluorescent sensors based on this unique heterocyclic moiety.[62] Owing to the strong coordination ability of the 2,2′-biimidazole moiety, metal ions are usually considered as the primary analytes, also with protons, anions and other biomolecules as the targets, to a lesser extent.

We first synthesized two conjugated polymers by Suzuki polycondensation from the derivatives of 2,2′-biimidazole and 3,6-carbazole (**CP-28** and **CP-29a**).[62a] Both of the polymers showed a blue emission peak, due to the presence of the carbazole-biimidazole unit, while **CP-29a** also had an emission band centered at 560 nm, which could be attributed to the additional carbazole-benzothiazole structure. Based on the

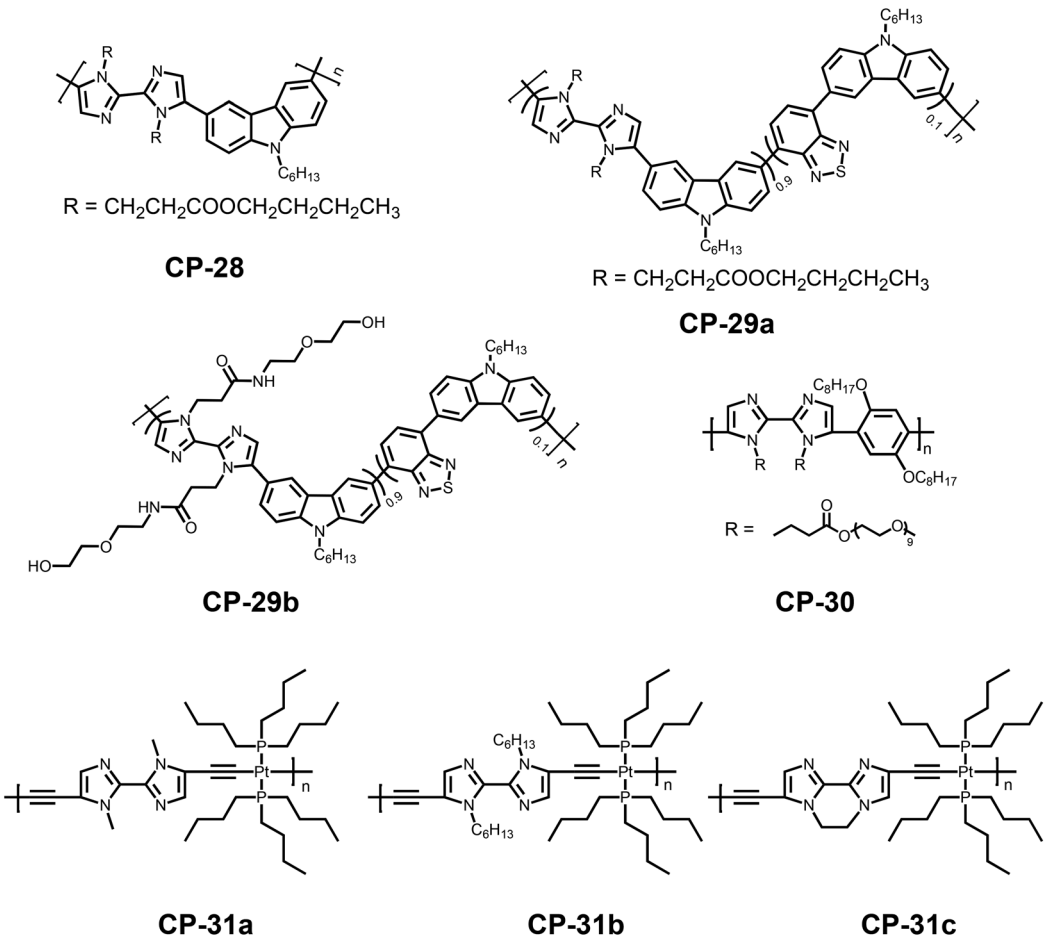

Fig. 15 Chemical structures of the representative 2,2-biimidazole-based CP sensors.

absorption peak of the carbazole-benzothiazole unit overlapping with the emission peak of the carbazole-biimidazole unit, it was found that an obvious Förster resonance energy transfer (FRET) process existed in **CP-29a**. The addition of Ag^+ ions induced a decrement in the fluorescence intensity of the blue emission peak for both of the polymers accompanied by a small red shift, likely because of both electron density variations on the backbone and chain aggregation induced by coordination (Fig. 16a). The fluorescence response of **CP-29s** to Ag^+ was somewhat different from that of **CP-28** in that the emission band at 560 nm showed a weaker fluorescence quenching because of the FRET process. As a result, the intensity ratio of two emission peaks gradually increases with the Ag^+ concentration with the fluorescence changing from reddish orange to yellow orange. Based on this significant response, Ag^+ could be readily distinguished from the other metal ions by the emission shift and ratiometric measurements (Fig. 16b). Subsequently, the complexes of **CP-28** and **CP-29a** with Ag^+ ions were also constructed as highly sensitive and selective fluorescent sensors for the detection of cysteine (Cys), thanks to the strong thiol–Ag^+ interactions (Fig. 16c and d). The detection limit was determined to be as low as 90 nM by a fluorimetric assay.

Despite the strongly hydrophobic conjugated backbone, interestingly, **CP-29a** exhibited strong orangish-red fluorescence emission in aqueous solutions after simple nanoprecipitation, benefiting from the aggregation-enhanced FRET activity. This endowed the polymer with extra function to sense electron deficient nitroaromatic molecules, based on the photo-induced electron transfer (PET) mechanism (Fig. 16e).[62b] The nanoparticles formed were fairly stable in dispersity and fluorescence intensity, and exhibited high sensitivity for the detection of picric acid with a K_{SV} of 3.4×10^4 M^{-1} and a detection limit of 5.1×10^{-7} M, as well as high selectivity over other nitroaromatic molecules. As the 2,2-biimidazole units were tightly embedded in nanoparticles, the detection process was free from the interference of metal ions, showing excellent advantages over previously reported methods (Fig. 15).

To further check the effect of the hydrophilicity of the side chains on the fluorescence of the polymer, **CP-29a** was subsequently ammonolyzed to obtain **CP-29b** with amphiphilic side chains.[62c] This new polymer could be dispersed in aqueous solutions and could form different aggregates in various solvents due to the strong π–π stacking interaction of the conjugated backbone. In dioxane–H_2O solutions, when the

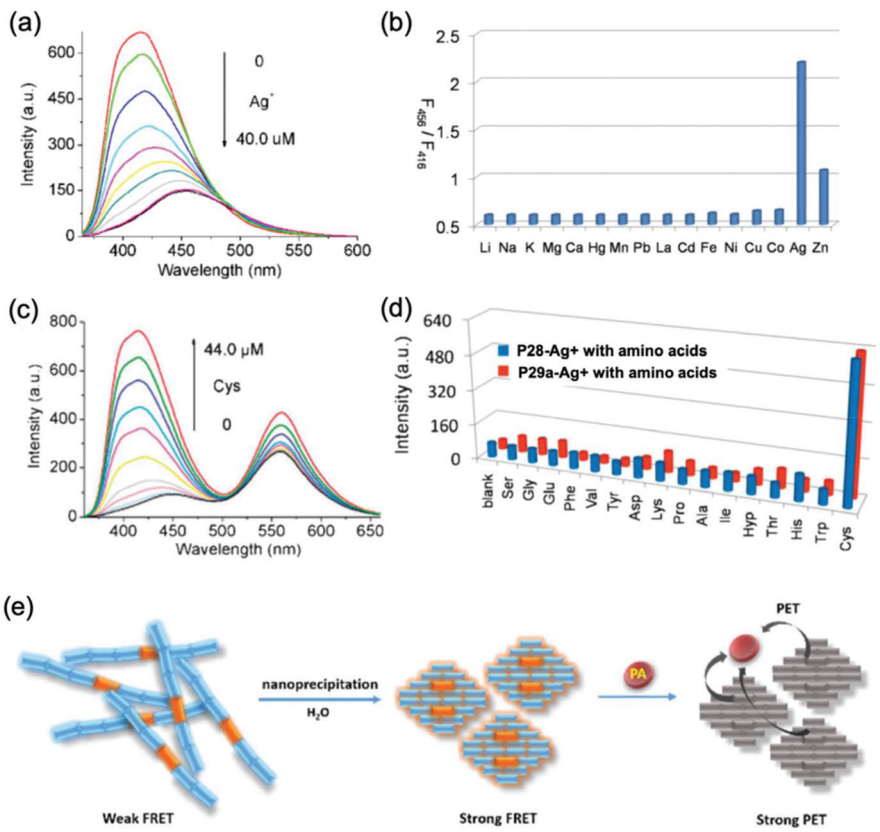

Fig. 16 (a) Fluorescence spectra of **CP-28** + Ag^+ in the presence of increasing Ag^+ concentrations; (b) intensity ratio $F_{560\ nm}/F_{416\ nm}$ of **CP-28** in the presence of indicated metal ions. [**CP28**] = 8.0 μM. λ_{ex} = 333 nm. (c) Fluorescence spectra of **CP-29a**–Ag^+ upon the titration of Cys; (d) amino acid selectivity profiles of **CP-29a**–Ag^+. [**CP29a**–Ag^+] = 8.0 μM. λ_{ex} = 333 nm;[62a] (e) schematic of fluorescence sensing of PA by **CP-29a** nanoparticles in aqueous solutions based on aggregation-enhanced FRET. Reproduced with permission from ref. 62*a* and *b*. Copyright 2018, The Royal Society of Chemistry.

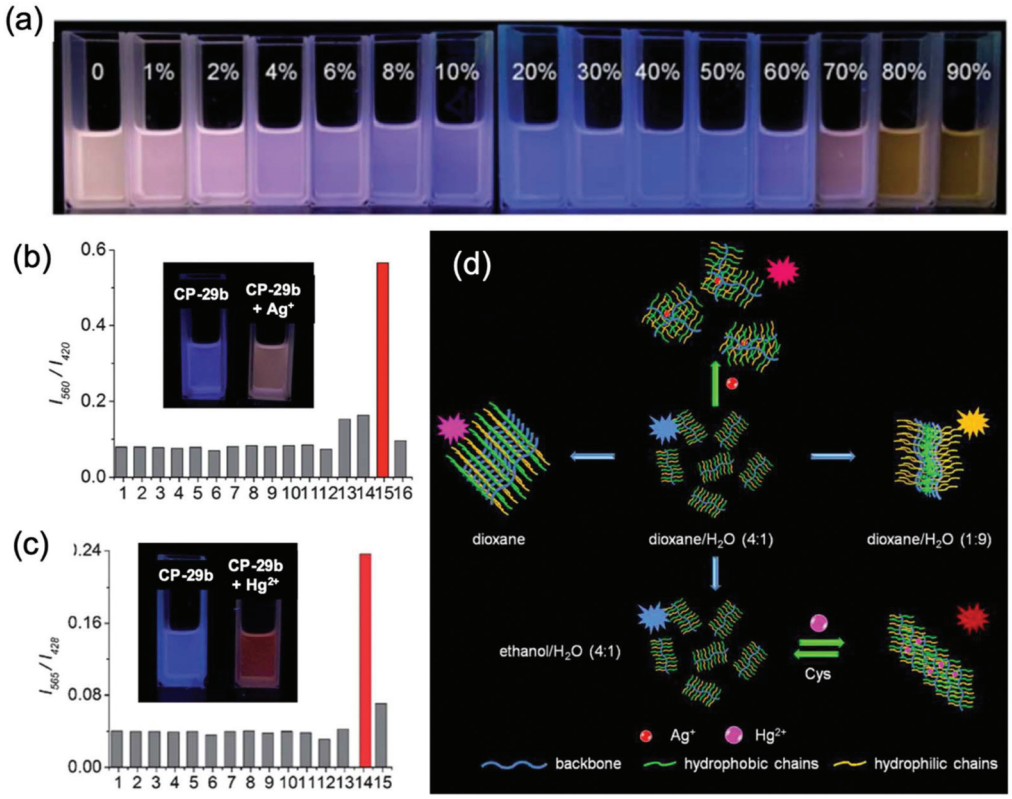

Fig. 17 (a) Fluorescence color changes, under a UV lamp, observed for **CP-29b** upon changing the water content from 0 to 90% in dioxane solution. (b) Selectivity profiles of **CP-29b** (8.0 μM) for sensing in MES (0.01 M) solution (dioxane–H_2O = 4 : 1, v/v, pH 6.0). Inset: Fluorescence color changes, under the UV lamp, observed upon addition of 10.0 equiv. of Ag^+; (c) selectivity profiles of **CP-29b** (8.0 μM) for sensing in MES (0.01 M) solution (ethanol–H_2O = 4 : 1, v/v, pH 6.0). Inset: Fluorescence color changes under the UV lamp; (d) schematic illustration of the aggregation-based multifunctional sensing platform with multicolor fluorescence response from amphiphilic **CP-29b**. For metal ions: 1, blank; 2, Na^+; 3, K^+; 4, Mg^{2+}; 5, Ca^{2+}; 6, Co^{2+}; 7, Ni^{2+}; 8, Zn^{2+}; 9, Cd^{2+}; 10, Pb^{2+}; 11, Mn^{2+}; 12, Cu^{2+}; 13, Fe^{3+}; 14, Hg^{2+}; 15, Ag^+; and 16, Cu^+. λ_{ex} = 338 nm. Reproduced with permission from ref. 62*c*. Copyright 2014, The Royal Society of Chemistry.

water content increased from 0 to 20%, because of a decrease in the aggregation degree, the emission peak at 560 nm gradually decreased while the emission peak at 420 nm exhibited a small enhancement. The fluorescence color variation from pink to blue could be distinctly observed with the naked eye. When the water content was further increased from 20% to 90%, the emission peak at 420 nm sharply decreased and the fluorescence intensity at 560 nm exhibited an obvious increment, because the polymer backbone and the hydrophobic side chains began to aggregate, and subsequently the FRET effect was greatly enhanced, accompanied by self-quenching. Simultaneously, the emission color variations from blue to orange could also be observed (Fig. 17a). Surprisingly, **CP-29b** exhibited significantly different sensing performance, but with high selectivity, in two different media. In dioxane/water (4 : 1, v/v) mixed solvent, the fluorescence of **CP-29b** turned into a purplish red color after the addition of Ag^+ (Fig. 17b), while Hg^{2+} and Cu^{2+} almost had no influence on the fluorescence. In parallel, when the detection medium chosen was ethanol/water (4 : 1, v/v), it showed a visually noticeable fluorescence response to Hg^{2+}, with high selectivity over other metal ions. Therefore, the structural design of the side chains has enormous impact on the fluorescence properties and sensing behaviors of the 2,2′-biimidazole-based conjugated polymers, as shown in Fig. 17c.

To explore further applications of conjugated polymers containing 2,2′-biimidazole moieties, we also used dialkoxy *p*-phenylene as the building units instead of 3,6-cabarzole groups, for the Suzuki polycondensation.[62*d*] As shown in Fig. 18, the fluorescence of the resulting polymer (**CP-30**) with PEG side chains could be strongly quenched by Cu^{2+} ions in aqueous solutions, with a K_{SV} of 3.3×10^5 M^{-1}. This indicated that the design of the conjugated backbone also has significant influence on the polymer's sensing properties, in accordance with the discovery related to 2,2′-bipyridine-based polymers. The polymer–Cu^{2+} complex was further developed as a highly efficient sensor for the detection of pyrophosphate anions (PPi), and the detection limit was determined to be 0.17 ppm. This work provided a new strategy for the development of PPi sensors. Later, it was found that the introduction of a branched structure to the conjugated main chain could enhance the sensitivity of the fluorescence sensing.[62*e*]

Wu and coworkers also developed a series of platinum(II) polymetallaynes with different 2,2-biimidazole-based organic

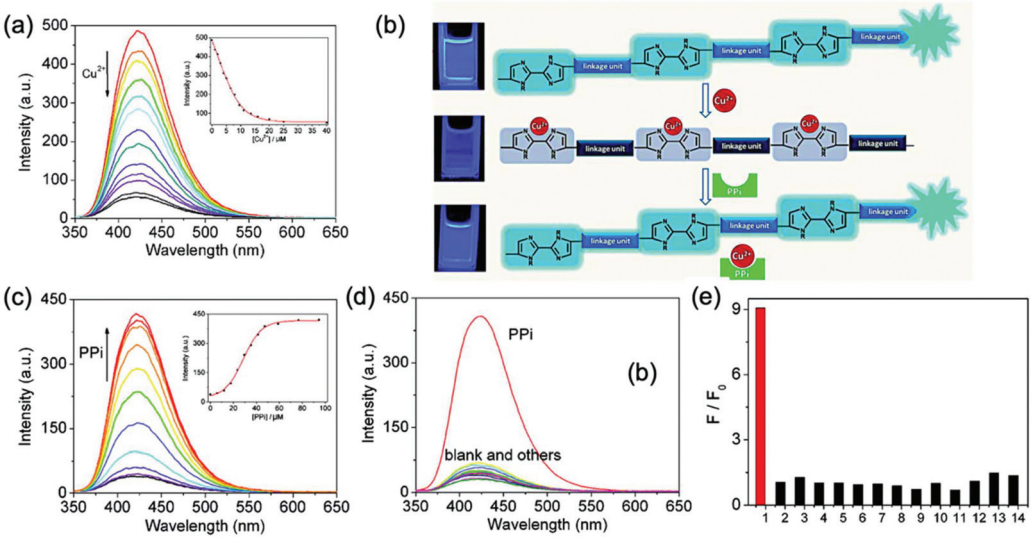

Fig. 18 (a) Fluorescence spectra of **CP-30** upon the titration of Cu^{2+} in DMF–HEPES (pH = 7.4, v/v = 4 : 1). Inset: Fluorescence intensity of **CP-30** as a function of the Cu^{2+} concentration. (b) Schematic representation of PPi sensors based on the fluorescence "on–off–on" of **CP-30**. (c) Fluorescence spectra of the **CP-30**–Cu^{2+} complex upon titration of PPi in DMF–HEPES (pH = 7.4, v/v = 4 : 1). Inset: Fluorescence intensity of the **CP-30**–Cu^{2+} complex as a function of the PPi concentration. (d) Fluorescence spectra of the **CP-30**–Cu^{2+} complex and (e) intensity ratios F/F_0 of the **P1**–Cu^{2+} complex in the presence of 40.0 μM PPi and 80.0 μM various anions in DMF–HEPES (pH = 7.4, v/v = 4 : 1). [**CP-30**] = 8.0 μM. [Cu^{2+}] = 20.0 μM. λ_{ex} = 338 nm. For anions: 1, PPi; 2, F^-; 3, Cl^-; 4, Br^-; 5, I^-; 6, NO_3^-; 7, HSO_4^-; 8, ClO_4^-; 9, AcO^-; 10, HCO_3^-; 11, CO_3^{2-}, 12, $H_2PO_4^-$; 13, HPO_4^{2-}; and 14, PO_4^{3-}. Reproduced with permission from ref. 62*d*. Copyright 2012, American Chemical Society.

spacers.[63] By adjusting both the configuration and the steric effect of the 2,2-biimidazole-based spacers, the sensing properties of the polymetallaynes can be tuned remarkably. The fluorescence signals for **CP-31a** and **CP-31c** were clearly quenched by Cu^{2+} ions with K_{SV} values determined to be 3.5 × 10^4 M^{-1} for **CP-31a** and 6.8 × 10^4 M^{-1} for **CP-31c**, respectively. However, the fluorescence of **CP-31b** was quite insensitive to Cu^{2+} ions (K_{SV} was 7.9 × 10^3 M^{-1}). Conferred by the locking effect of the ethylene unit, a good coplanar feature of the biimidazole units existed in **CP-31c**. This configuration favored its binding with Cu^{2+}, which induced the quenching of the fluorescence. The coordination of the 2,2-biimidazole units with Cu^{2+} ions in **CP-31a** and **CP-31b**, however, involved the rotation of the imidazole rings from the low-energy optimized configuration with two alkyl groups in the *trans* pattern to the coplanar configuration with two alkyl groups in the *cis* form. The bulky hexyl groups in the biimidazole unit of **CP-31b** exhibited a higher steric effect than the small methyl groups in **CP-31a**. This large steric effect restricted the coordination of the biimidazole unit in **CP-31b** with Cu^{2+}, thus showing inferior sensitivity.

This year, Geng and coworkers prepared two biimidazole-based porous organic polymers for sensing both I_2 and nitroaromatic compounds (*e.g.*, picric acid and *p*-nitrophenol) *via* fluorescence quenching, and in particular, one polymer exhibited high sensitivity toward iodine with a K_{SV} of 1.16 × 10^4 L mol^{-1} and a detection limit of 0.13 nM.[64] Despite the promising results obtained from biimidazole moiety-derivatized polymer sensors, the publications are still much fewer than those based on bipyridine group-incorporated polymers. In other words, there are still many opportunities for developing more efficient chemosensors and exploring new applications, by means of chemical structure design on both the biimidazole unit and polymer backbone/side group, as well as the investigation of structure–property relationships.

5. CP chemosensors based on fused N-heterocycles

In addition to the typical pyridine and imidazole-derived receptor units, fused heterocycles with nitrogen atoms were also employed to construct efficient fluorescent sensors. In this part, the representative fused heterocycles including quinine, 1,10-phenanthrolene and their derivatives will be introduced regarding their sensing performance in conjugated polymers.

Quinine, as a key member of various fused heterocycles, has evoked much interest in recent decades as a result of its broad applications in medicine, organic light emitting diodes, light harvesting materials, *etc*.[65] Its function in CP fluorescent sensors has also been studied. For instance, in 2002, two polyquinolines including **CP-32** were reported by Wang *et al.* Interestingly, most of the metal ions had no influence on the fluorescence of **CP-32** except that Ag^+ induced a distinct quenching. Amplified fluorescence quenching arises, mainly from the Ag^+ induced intermolecular aggregation.[66a] 8-Quinolinol, as one of the most important derivatives of quinine, possesses a superior coordination ability toward metal ions, making it a good receptor to fabricate novel che-

mosensors.[66b] Yamamoto and co-workers synthesized two conjugated polymers with 8-quinolinol on their main chain (**CP-33a** and **CP-33b**), which exhibited strong affinity to certain metal ions.[67] Zn^{2+} could moderately quench the fluorescence of **CP-33b**; in parallel, Al^{3+} led to the emergence of a new peak at 500 nm, while Pd^{2+} almost fully quenched the fluorescence. A similar phenomenon was also observed for the CP sensors bearing 1,10-phenanthroline groups, developed by the same group.[68] The position of the substituent on 8-quinolinol has an obvious influence on the sensitivity of metal ion detection. An electron withdrawing ethynyl group substituted at the *ortho*-position induced a higher acidity of the hydroxyl group in the 8-quinolinol unit. This made the resulting polymer **CP-33a** more sensitive compared with **CP-33b**, which has substituted groups at the *meta*-position. There are other systems containing 8-quinolinol units also reported with a similar phenomenon.[69]

The functional groups attached to the backbones play an important role in the response behaviors of the polymers.[70] **CP-34** has a bromoalkyl functional group linked to the hydroxyl group of the 8-quinolinol unit, and its fluorescence was hardly quenched by Cu^{2+},[70a] whereas, once the group was replaced with imidazole or detached, the resulting polymers **CP-35** and **CP-36** immediately showed a strong affinity to Cu^{2+} ions, and their emissions were dramatically quenched. The metal–polymer complexes were further investigated for their sensing properties to amino acids. Similarly, the type of substituent group of the 8-quinolinol unit also led to different performances in the detection. The addition of glycine into the **CP-35**–Cu^{2+} system induced a recovery of the quenched emission; in contrast, the same action could not facilitate any variation in the optical properties of the **CP-36**–Cu^{2+} complex. The reason is that 8-hydroxyquinoline (8HQ) is much strongly coordinated to Cu^{2+}, which prevents it from being snatched by amino acids (Fig. 19).

Liu and co-workers synthesized a polymer with quinoline substituted side chains (**CP-37**).[71a] The polymer **CP-37** is weakly emissive in DMSO because of photo-induced electron transfer from electron-rich groups (OH and NH) to the electron deficient unit. Among various metal ions, only the addition of Hg^{2+} caused an obvious fluorescence enhancement, showing good selectivity (Fig. 20). This is one of the few examples that transition metal ions can switch on the emission of CP sensors. In general, publications on fluorescent sensors based on polymeric 8-quinolinol remain limited, compared to those based on small molecules.[71b–g]

As one of the most significant building blocks for fluorescent supramolecular architectures, metallo-chelates and pharmaceutics, 1,10-phenanthroline possesses many attractive structural properties such as high rigidity, planarity and strong coordinating capacity.[72] This makes it an entropically better chelating molecule than the commonly used 2,2′-bipyridine, endowing it with a fascinating unit for constructing CP chemosensors.[73] Yamamoto and coworkers prepared a π-conjugated polymer (**CP-38**) containing a 1,10-phenanthroline unit, and studied its optical properties in the presence of various metal ions.[74] Numerous metal ions can induce the variation of the fluorescence properties. The changes can be categorized into

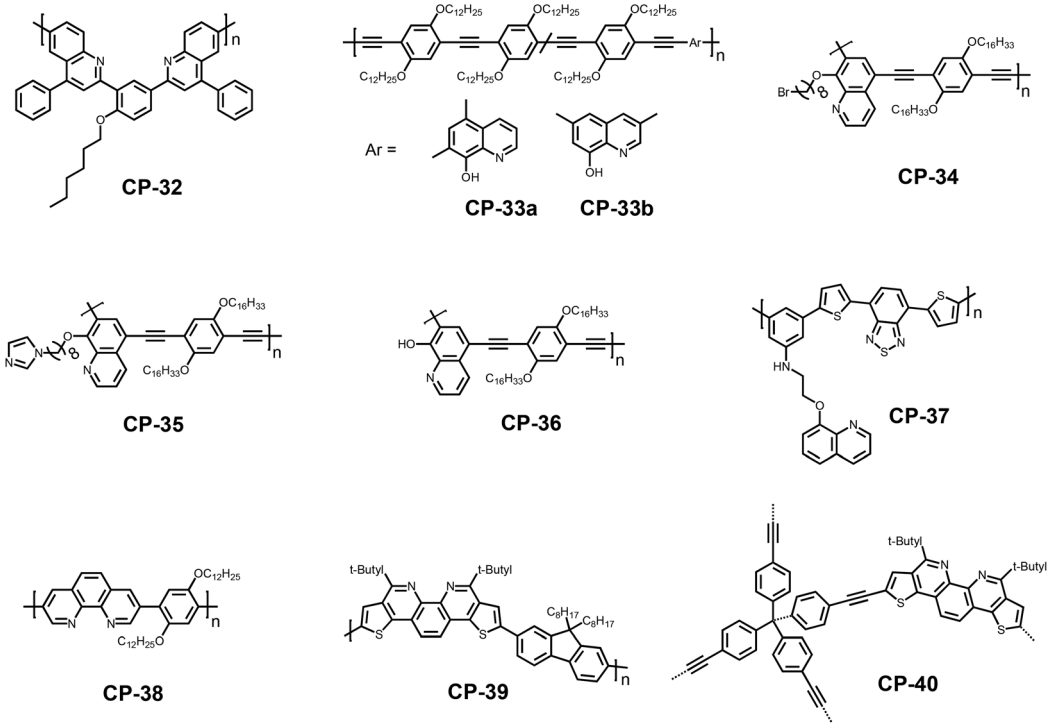

Fig. 19 Chemical structures of the representative CP chemosensors based on fused N-heterocycles.

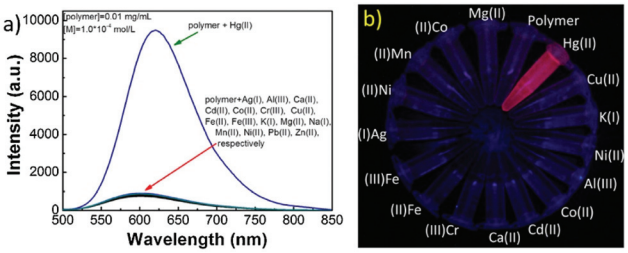

Fig. 20 Fluorescence sensing properties of **CP-37** with metal ions in DMSO. (a) Interactions of the polymer (0.01 mg mL^{-1}) with various metal ions (1.0 × 10^{-4} mol L^{-1}); and (b) emission color changes of polymer solutions in the presence of various metal ions. Reproduced with permission from ref. 71*a*. Copyright 2017, Elsevier.

two groups: (i) a relatively small degree of red-shift; and (ii) a relatively large red-shift and quenching due to an energy transfer from the polymer backbone to the metal complexes.

Zhu and coworkers[75] fabricated a dipyrido[3,2-*a*:2,3-*c*]phenazine (dppz) based selective metal ion sensor with ultrahigh sensitivity. The original polymer displayed red fluorescence in THF solution, while a drastic intensity decrease was observed for Ni^{2+} with a detection limit as low as 6.5 × 10^{-12} M. The observed fluorescence quenching is mainly ascribed to the chelation between the polymer and Ni^{2+}, forming a low-lying metal–ligand charge transfer state. It was found that there were three linear regions in the Stern–Volmer plot. The Stern–Volmer constants were determined to be 2.57 × 10^{9} M^{-1} [(0.0005–0.004) × 10^{-8} M], 2.63 × 10^{7} M^{-1} [(0.03–0.3) × 10^{-8} M], and 8.27 × 10^{6} M^{-1} [(1–20) × 10^{-8} M]. Although the exact nature was not clear, an upwardly positive deviation at higher concentrations indicated the presence of combined quenching actions.

Recently, Chen and coworkers designed a thiophene-fused derivative of 1,10-phenanthroline with a π-extended structure, and used it to synthesize a series of new conjugated polymers as fluorescent chemosensors.[76] For example, the emission of **CP-39** was weakened by Mn^{2+}, while Cu^{2+}, Al^{3+}, and Co^{2+} caused a more significant decrease in intensity accompanied by a red-shift in emission.[76*a*] Complete quenching was observed for Fe^{3+} and Fe^{2+} because of the strong coordination with the 1,10-phenanthroline group and the amplification effect of the CP backbone (Fig. 21). Utilizing this S,N-heteroatom unit, a π-conjugated microporous polymer (**CP-40**) was prepared by Sonogashira polymerization.[76*b*] The introduction of S,N-heteroacenes not only furnished the polymer with high porosity but also endowed it with a unique sensing ability. The electron deficient nitro aromatic compounds could quench the fluorescence of the polymer, especially for picric acid (PA), through a donor–accepter energy transfer mechanism. The S, N-heteroatoms and porous structures of **CP-40** enabled it to load a high level of silver nanoparticles, thus achieving additional antimicrobial activities. Note that this review did not include all of the CP sensors based on N-heterocycles, but only selected the most representative examples. Thus, there are still certain amounts of CP sensors based on other heterocycles, which could also be of interest to the readers, yet not shown here.

6. Conclusions and perspectives

Over the past more than two decades of time, significant progress has been achieved in the research of π-conjugated polymer-based fluorescent sensors, especially for the ones containing aromatic N-heterocyclic moieties. (i) Thanks to the significant signal amplifying activity or molecular wire effect, they usually displayed ultrahigh sensitivity to the analytes with the detection limit in the micro- to nanomolar or even picomolar range. In particular, to interact with transition/heavy metal ions, the Stern–Volmer quenching constant (K_{SV}) could be as high as 10^{5}–10^{9} M^{-1}, much higher than those of the chemical sensors based on small molecules. Accordingly, the resulting metal–polymer complexes also exhibited high sensitivity to the target analytes, such as anions, amino acids, *etc*. (ii) Benefiting from various N-heterocyclic groups available that can be introduced to the polymer backbone or side chains, the sensing performance can be manipulated by tailoring the receptor type, main chain design and side group functionalization, and consequently the sensing applications can be greatly expanded. (iii) More and more conjugated polymer-based sensors have been developed for carrying out the detection in aqueous solutions,[21,28,44*c*,51,62*b*,*c*] so that the application becomes much more realistic than before. This is of high

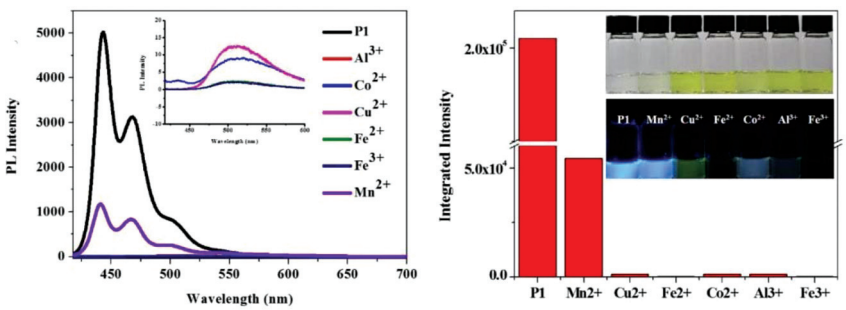

Fig. 21 Fluorescence response of **CP-39** to metal ions in chloroform. Insets show the pictures of polymer solutions treated with metal ions (under natural light or 365 nm UV light).[76*a*] Reproduced with permission from ref. 76*a*. Copyright 2016, American Chemical Society.

importance for biomedical applications, especially for diagnostics and bioimaging.

Despite the distinguished achievements, these polymer sensors are still not in use in real life as molecular sensors, and some of them have been commercialized for applications in life sciences. In order to achieve similar targets, certain shortcomings need to be overcome: (i) in general, the selectivity of the sensors based on N-heterocyclic moieties toward metal ions remains unsatisfactory, owing to the non-specific binding, especially for the mono-aromatic ring receptor, such as pyridine or imidazole. However, the recent strategy incorporating additional aromatic rings with electron donating elements such as sulfur could be a potential method to tackle this issue, with the help of synergistic effects from multiple chelating groups. (ii) Most of the metal ion sensors based on heterocyclic conjugated polymers are based on the fluorescence quenching approach, which is not optimal for real applications, given the potential interference from the environment and machine background. Instead, the polymer sensors with emission-shifts as responses are highly desired, and they can give a ratiometric fluorescence signal.[77] (iii) Although certain examples have been reported for sensing in aqueous solutions, the detection in a pure water environment remains limited. The introduction of water-soluble side chains such as PEG or ionic groups could be an efficient method; however, it can also cause the variation of the sensing performance. Thus, the structure–property relationships should be carefully evaluated.

In fact, there is still large space to be explored for the design of heterocyclic conjugated polymers as efficient fluorescent sensors. For example, in the case of 2,2′-biimidazole, only the simplest derivatives have been introduced into polymer systems, with a number of possibilities of further chemical modifications not taken into consideration. On the other hand, new light-emission mechanisms including aggregation-induced emission (AIE),[78] through-space charge transfer (TSCT)[79] and thermally activated delayed fluorescence (TADF),[80] have emerged as efficient tools to design new fluorescent materials. This could provide tremendous new opportunities for the fabrication of conjugated polymer sensors. However, compliance with the rules in biomedical applications such as diagnostics and drug delivery[81] is still an unmet need for heterocyclic conjugated polymer sensors. Note that computational modeling and simulation have been widely used in the design of molecular chemical sensors,[71g] and they could be also of high importance for synthesizing polymer sensors, despite the possible high working load from the complex polymeric structure and long polymer chains. Nowadays, artificial intelligence is being used in the field of drug discovery and chemical synthesis route development, and is changing our lives unprecedentedly. Therefore, the design of conjugated polymer sensors would be much more efficient in the near future, supported by the above modern technologies.

Conflicts of interest

There are no conflicts to declare.

Acknowledgements

This work is dedicated to Prof. Ruke Bai for his achievement in polymer chemistry, on the occasion of his recent retirement, from the University of Science and Technology of China.

The authors thank the National Natural Science Foundation of China (Grant No. 51803090), Natural Science Foundation of Jiangsu (Grant No. BK20181025 and BK20191022), and Introducing Talents Fund of Nanjing Institute of Technology (YKJ201807 and YKJ201808) for financial support. Y. Bao acknowledges the financial support from the Swiss National Science Foundation (SNF Spark grant, No. 190313) and Fondation Claude et Giuliana (No. 1-005137).

References

1 P. Gründler, *Chemical Sensors: An Introduction for Scientists and Engineers*, Springer, New York, 2007.
2 (*a*) D. Wu, A. C. Sedgwick, T. Gunnlaugsson, E. U. Akkaya, J. Yoon and T. D. James, *Chem. Soc. Rev.*, 2017, **46**, 7105–7123; (*b*) F. Wang, L. Wang, X. Q. Chen and J. Yoon, *Chem. Soc. Rev.*, 2014, **43**, 4312–4324.
3 A. Popov, H. Chen, O. N. Kharybin, E. N. Nikolaev and R. G. Cooks, *Chem. Commun.*, 2005, 1953–1955.
4 J. M. Sylvia, J. A. Janni, J. D. Klein and K. M. Spencer, *Anal. Chem.*, 2000, **72**, 5834–5840.
5 (*a*) E. Wallis, T. M. Griffin, N. Popkie, M. A. Eagan, R. F. McAtee, D. Vrazel and J. McKinly, *Proc. SPIE-Int. Soc. Opt. Eng.*, 2005, **5795**, 54–64; (*b*) G. A. Eiceman and J. A. Stone, *Anal. Chem.*, 2004, **76**, 390A–397A.
6 (*a*) S. H. Park, N. Kwon, J. H. Lee, J. Yoon and I. Shin, *Chem. Soc. Rev.*, 2020, **49**, 143–179; (*b*) D. Wu, L. Y. Chen, Q. L. Xu, X. Q. Chen and J. Yoon, *Acc. Chem. Res.*, 2019, **52**(8), 2158–2168.
7 (*a*) Y. Z. Li, S. J. Qi, C. C. Xia, Y. H. Xu, G. Y. Duan and Y. Q. Ge, *Anal. Chim. Acta*, 2019, **1077**, 243–248; (*b*) Y. K. Yue, F. J. Huo, F. Q. Cheng, X. J. Zhu, T. Mafirefi, R. M. Strongin and C. X. Yin, *Chem. Soc. Rev.*, 2019, **48**, 4155–4177.
8 W. Sun, S. G. Guo, C. Hu, J. L. Fan and X. J. Peng, *Chem. Rev.*, 2016, **116**, 7768–7817.
9 B. R. Eggins, *Chemical Sensors and Biosensors*, Wiley, West Sussex, 2008, vol. 28.
10 (*a*) S. W. Thomas, G. D. Joly and T. M. Swager, *Chem. Rev.*, 2007, **107**, 1339–1386; (*b*) C. J. Qin, X. F. Wu, B. X. Gao, H. Tong and L. X. Wang, *Macromolecules*, 2009, **42**, 5427–5429; (*c*) X. F. Wu, B. W. Xu, H. Tong and L. X. Wang, *Macromolecules*, 2010, **43**, 8917–8923; (*d*) B. W. Xu, X. F. Wu, H. B. Li, H. Tong and L. X. Wang, *Macromolecules*, 2011, **44**, 5089–5092; (*e*) X. F. Wu, B. W. Xu, H. Tong and L. X. Wang, *Macromolecules*, 2011, **44**, 4241–4248; (*f*) Q. Zhou and T. M. Swager, *J. Am. Chem. Soc.*, 1995, **117**(50), 12593–12602; (*g*) S. Rochat and T. M. Swager, *ACS Appl. Mater. Interfaces*, 2013, **5**, 4488–

4502; (*h*) T. M. Swager, *Macromolecules*, 2017, **50**(13), 4867–4886.

11 (*a*) L. H. Feng, C. L. Zhu, H. X. Yuan, L. B. Liu, F. T. Lv and S. Wang, *Chem. Soc. Rev.*, 2013, **42**, 6620–6633; (*b*) A. I. Gopalan, S. Komathi, N. Muthuchamy, K. P. Lee, M. J. Whitcombe, L. Dhana and G. S. Anand, *Prog. Polym. Sci.*, 2019, **88**, 1–129; (*c*) H. Zhou, M. H. Chua, B. Z. Tang and J. W. Xu, *Polym. Chem.*, 2019, **10**, 3822–3840; (*d*) W. B. Wu, G. C. Bazan and B. Liu, *Chem*, 2017, **2**, 760–790; (*e*) B. Wang, B. N. Queenan, S. Wang, K. P. R. Nilsson and G. C. Bazan, *Adv. Mater.*, 2019, **31**, 1806701; (*f*) R. Sakai, *Polym. J.*, 2016, **48**, 59–65; (*g*) S. Rochat and T. M. Swager, *ACS Appl. Mater. Interfaces*, 2013, **5**, 4488–4502.

12 (*a*) S. J. Liu, Y. Chen, W. J. Xu, Q. Zhao and W. Huang, *Macromol. Rapid Commun.*, 2012, **33**, 461–480; (*b*) M. T. Nguyen, R. A. Jones and B. J. Holliday, *Coord. Chem. Rev.*, 2018, **377**, 237–258; (*c*) B. Wang and M. R. Wasielewski, *J. Am. Chem. Soc.*, 1997, **119**, 12–21.

13 (*a*) S. Khatua and M. Schmittel, *Org. Lett.*, 2013, **15**(17), 4422–4425; (*b*) O. Kotova, S. Comby and T. Gunnlaugsson, *Chem. Commun.*, 2011, **47**, 6810–6812; (*c*) Z. H. Lin, S. J. Ou, C. Y. Duan, B. G. Zhang and Z. P. Bai, *Chem. Commun.*, 2006, 624–626.

14 (*a*) C. Y. K. Chan, J. W. Y. Lam, C. Deng, X. J. Chen, K. S. Wong and B. Z. Tang, *Macromolecules*, 2015, **48**(4), 1038–1047; (*b*) M. Wang, G. X. Zhang, D. Q. Zhang, D. B. Zhu and B. Z. Tang, *J. Mater. Chem.*, 2010, **20**, 1858–1867.

15 (*a*) S. Y. Lim, K. H. Hong, D. Kim, H. Kwon and H. J. Kim, *J. Am. Chem. Soc.*, 2014, **136**, 7018–7025; (*b*) Y. K. Yue, F. J. Huo, P. Yue, X. M. Meng, J. C. Salamanca, J. O. Escobedo, R. M. Strongin and C. X. Yin, *Anal. Chem.*, 2018, **90**(11), 7018–7024; (*c*) H. Zhang, L. Z. Xu, W. Q. Chen, J. Huang, C. S. Huang, J. R. Sheng and X. Z. Song, *ACS Sens.*, 2018, **12**, 2513–2517.

16 (*a*) S. Y. Li, L. H. Liu, H. Cheng, B. Li, W. X. Qiu and X. Z. Zhang, *Chem. Commun.*, 2015, **51**, 14520–14523; (*b*) K. Y. Tan, C. Y. Li, Y. F. Li, J. J. Fei, B. Yang, Y. J. Fu and F. Li, *Anal. Chem.*, 2017, **89**, 1749–1756; (*c*) J. Yin, Y. Kwon, D. Kim, D. Lee, G. Kim, Y. Hu, J. H. Ryu and J. Yoon, *J. Am. Chem. Soc.*, 2014, **136**, 5351–5358.

17 (*a*) C. Kaes, A. Katz and M. W. Hosseini, *Chem. Rev.*, 2000, **100**, 3553–3590; (*b*) Y. Liu, S. W. Zhang, Q. Miao, L. F. Zheng, L. L. Zong and Y. X. Cheng, *Macromolecules*, 2007, **40**, 4839–4847; (*c*) Y. Liu, Q. Miao, S. W. Zhang, X. B. Huang, L. F. Zheng and Y. X. Cheng, *Macromol. Chem. Phys.*, 2008, **209**, 685–694; (*d*) J. Pei, A. L. Ding, W. L. Yu and Y. H. Lai, *Macromol. Rapid Commun.*, 2002, **23**, 21–25.

18 W. A. Braunecker and K. Matyjaszewski, *Prog. Polym. Sci.*, 2007, **32**, 93–146.

19 (*a*) E. C. Constable and C. E. Housecroft, *Molecules*, 2019, **24**, 3951–3988; (*b*) D. A. Turchetti, P. C. Rodrigues, L. S. Berlim, C. Zanlorenzi, G. C. Faria, T. D. Z. Atvars, W. H. Schreiner and L. C. Akcelrud, *Synth. Met.*, 2012, **162**, 35–43.

20 C. Y. Yu, P. Y. Chen, Y. H. Lin, P. J. Ciou and J. Appl, *Polym. Sci.*, 2015, **132**, 42795–42802.

21 C. F. Xing, Z. Q. Shi, M. H. Yu and S. Wang, *Polymer*, 2008, **49**, 2698–2703.

22 R. C. Smith, A. G. Tennyson, M. H. Lim and S. J. Lippard, *Org. Lett.*, 2005, **7**, 3573–3575.

23 S. He, A. A. Buelt, J. M. Hanley, B. P. Morgan, A. G. Tennyson and R. C. Smith, *Macromolecules*, 2012, **45**, 6344–6352.

24 C. Li, C. Zhou, H. Zheng, X. Yin, Z. Zuo, H. Liu and Y. Li, *J. Polym. Sci., Part A: Polym. Chem.*, 2008, **46**, 1998–2007.

25 T. Hosomi, H. Masai, T. Fujihara, Y. Tsuji and J. Terao, *Angew. Chem., Int. Ed.*, 2016, **55**, 13427–13431.

26 (*a*) X. Y. Zhao, M. R. Pinto, L. M. Hardison, J. Mwaura, J. Muller, H. Jiang, D. Witker, V. D. Kleiman, J. R. Reynolds and K. S. Schanze, *Macromolecules*, 2006, **39**, 6355–6366; (*b*) M. F. Gui, J. Jiang, X. Wang, Y. X. Yan, S. Q. Li, X. L. Xiao, T. B. Liu, T. G. Liu and Y. Feng, *Sens. Actuators, B*, 2017, **243**, 696–703; (*c*) I. Welterlich and B. Tieke, *Macromolecules*, 2011, **44**, 4194–4203; (*d*) M. Bender, K. Seehafer, M. Findt and U. H. F. Bunz, *RSC Adv.*, 2015, **5**, 96189–96193.

27 K. Seehafer, M. Bender and U. H. F. Bunz, *Macromolecules*, 2014, **47**, 922–927.

28 K. Seehafer, M. Bender, S. T. Schwaebel and U. H. F. Bunz, *Macromolecules*, 2014, **47**, 7014–7020.

29 S. K. Samanta, N. Dey, N. Kumari, D. Biswakarma and S. Bhattacharya, *ACS Sustainable Chem. Eng.*, 2019, **7**, 12304–12314.

30 X. D. Lou, Y. Zhang, S. Li, D. X. Ou, Z. M. Wan, J. G. Qin and Z. Li, *Polym. Chem.*, 2012, **3**, 1446–1452.

31 B. Liu, Y. Y. Bao, F. F. Du, J. Tian and R. K. Bai, *Chem. Commun.*, 2011, **47**, 1731–1733.

32 H. M. Huang, K. M. Wang, W. H. Tan, D. An, X. H. Yang, S. S. Huang, Q. G. Zhai, L. J. Zhou and Y. Jin, *Angew. Chem.*, 2004, **116**, 5753–5756.

33 B. Liu, H. G. Dai, Y. Y. Bao, F. F. Du, J. Tian and R. K. Bai, *Polym. Chem.*, 2011, **2**, 1699–1705.

34 B. Liu, Y. Y. Bao, H. Wang, F. F. Du, J. Tian, Q. B. Li, T. S. Wang and R. K. Bai, *J. Mater. Chem.*, 2012, **22**, 3555–3561.

35 A. Wild, A. Winter, F. Schlutter and U. S. Schubert, *Chem. Soc. Rev.*, 2011, **40**, 1459–1511.

36 (*a*) J. M. Cole, K. S. Low and Y. Gong, *ACS Appl. Mater. Interfaces*, 2015, **7**, 27646–27653; (*b*) S. Fantacci, E. Ronca, F. D. Angelis and J. Phys, *Chem. Lett.*, 2014, **5**, 375–380; (*c*) S. S. M. Fernandes, M. Belsley, C. Ciarrocchi and M. Licchelli, *Dyes Pigm.*, 2018, **150**, 49–58; (*d*) S. Ghosh, G. K. Chaitanya and K. Bhanuprakash, *Inorg. Chem.*, 2006, **45**, 7600–7611; (*e*) H. Kusama, *J. Photochem. Photobiol., A*, 2017, **344**, 134–142.

37 (*a*) S. Kanagaraj, A. Puthanveedu and Y. Choe, *Adv. Funct. Mater.*, 2019, 1907126; (*b*) H. J. Bolink, L. Cappelli, E. Coronado and P. Gavina, *Inorg. Chem.*, 2005, **44**, 5966–5968.

38 (*a*) I. Eryazici, C. N. Moorefield and G. R. Newkome, *Chem. Rev.*, 2008, **108**, 1834–1895; (*b*) M. T. Gabr and F. C. Pigge, *Inorg. Chem.*, 2018, **57**, 12641–12649.
39 Z. Lin, N. C. Thacker, T. Sawano, T. Drake, P. Ji, G. Lan, L. Cao, S. Liu, C. Wang and W. Lin, *Chem. Sci.*, 2018, **9**, 143–151.
40 C. Y. Wei, Y. He, X. D. Shi and Z. G. Song, *Coord. Chem. Rev.*, 2019, **385**, 1–19.
41 M. Kimura, T. Horai, K. Hanabusa and H. Shirai, *Adv. Mater.*, 1998, **10**, 459–462.
42 (*a*) Q. Chu and Y. Pang, *J. Polym. Sci., Part A: Polym. Chem.*, 2006, **44**, 2338–2345; (*b*) A. R. Rabindranath, A. Maier, M. Schafer and B. Tieke, *Macromol. Chem. Phys.*, 2009, **210**, 659–668.
43 Y. Zhang, C. B. Murphy and W. E. Jones, *Macromolecules*, 2002, **35**, 630–636.
44 (*a*) R. S. Juang, H. W. Wen, M. T. Chen and P. C. Yang, *Sens. Actuators, B*, 2016, **231**, 399–411; (*b*) V. Banjoko, Y. Q. Xu, E. Mintz and Y. Pang, *Polymer*, 2009, **50**, 2001–2009; (*c*) A. Sil, S. N. Islam and S. K. Patra, *Sens. Actuators, B*, 2018, **254**, 618–628; (*d*) X. Y. Wang, Q. Q. Lin, S. Ramachandran, G. Pembouong, R. B. Pansu, I. Leray, B. Lebental and G. Zucchi, *Sens. Actuators, B*, 2019, **286**, 521–532; (*e*) P. C. Yang, H. W. Wen, C. W. Huang and Y. N. Zhu, *RSC Adv.*, 2016, **6**, 87680–87689; (*f*) P. C. Yang, S. Q. Li, Y. H. Chien, T. L. Tao, R. Y. Huang and H. Y. Chen, *Polymer*, 2017, **9**, 427–442.
45 L. Zhang, X. M. Peng, G. L. V. Damu, R. X. Geng and C. H. Zhou, *Med. Res. Rev.*, 2014, **34**, 340–437.
46 P. Molina, A. Tarraga and F. Oton, *Org. Biomol. Chem.*, 2012, **10**, 1711–1724.
47 H. A. Ho and M. Leclerc, *J. Am. Chem. Soc.*, 2003, **125**, 4412–4413.
48 (*a*) X. H. Zhou, J. C. Yan and J. Pei, *Macromolecules*, 2004, **37**, 7078–7080; (*b*) A. S. Castillo, M. C. Robles and R. Mallavia, *Chem. Commun.*, 2010, **46**, 1263–1265; (*c*) G. Xiang, W. Cui, S. Lin, L. Wang, H. Meier, L. Li and D. Cao, *Sens. Actuators, B*, 2013, **186**, 741–749; (*d*) I. K. Spiliopoulos, *Polym. Int.*, 2019, **68**, 1033–1041; (*e*) A. Parthasarathy, H. C. Pappas, E. H. Hill, Y. Huang, D. G. Whitten and K. S. Schanze, *ACS Appl. Mater. Interfaces*, 2015, **7**(51), 28027–28034.
49 Z. A. Li, X. D. Lou, H. B. Yu, Z. Li and J. G. Qin, *Macromolecules*, 2008, **41**, 7433–7439.
50 (*a*) Q. Zeng, P. Cai, Z. Li, J. G. Qin and B. Z. Tang, *Chem. Commun.*, 2008, 1094–1096; (*b*) Q. Zeng, C. K. W. Jim, J. W. Y. Lam, Y. Dong, Z. Li, J. G. Qin and B. Z. Tang, *Macromol. Rapid Commun.*, 2009, **30**, 170–175.
51 C. F. Xing, M. H. Yu, S. Wang, Z. Q. Shi, Y. L. Li and D. B. Zhu, *Macromol. Rapid Commun.*, 2007, **28**, 241–245.
52 D. Giri, A. Bankura and S. K. Patra, *Polymer*, 2018, **158**, 338–353.
53 (*a*) S. A. Rommel, D. Sorsche, M. Fleischmann and S. Eau, *Chem. – Eur. J.*, 2017, **23**, 18101–18119; (*b*) S. Liang, Y. M. Nie, S. H. Li, J. L. Zhou and J. Yan, *Molecules*, 2019, **24**, 806–819.
54 H. Debus, *Liebigs Ann. Chem.*, 1858, **107**, 199.
55 H. M. Zhang, X. G. Yan, J. Zhao, X. L. Yang, Z. Huang, G. J. Zhou and Y. Wu, *RSC Adv.*, 2015, **5**, 88758–88766.
56 (*a*) Y. C. Chen, Y. T. Kuo and T. H. Ho, *Photochem. Photobiol. Sci.*, 2019, **18**, 190–197; (*b*) A. F. Henwood, S. Evariste, A. M. Z. Slawin and E. Z. Colman, *Faraday Discuss.*, 2014, **174**, 165–182.
57 (*a*) S. J. S. Franchi, R. A. de Souza, A. E. Mauro, I. Z. Carlos, L. C. de Abreu Ribeiro, F. V. Rocha and A. V. de Godoy-Netto, *Acta Chim. Slov.*, 2018, **65**, 547–553; (*b*) H. Q. Shen, B. Wu, H. P. Xie and Y. G. Zhou, *Org. Lett.*, 2019, **21**(8), 2712–2717.
58 S. Matsumoto, Y. Zhao and M. Akazome, *Heterocycles*, 2014, **88**, 13–25.
59 (*a*) Y. Cui, H. J. Mo, J. C. Chen, Y. L. Niu, Y. R. Zhong, K. C. Zheng and B. H. Ye, *Inorg. Chem.*, 2007, **46**, 6427–6436; (*b*) A. Maiboroda, G. Rheinwald and H. Lang, *Inorg. Chem. Commun.*, 2001, **4**, 381–383; (*c*) M. Tadokoro and K. Nakasuji, *Coord. Chem. Rev.*, 2000, **198**, 205–218; (*d*) M. Tadokoro, T. Shiomi, K. Isobe and K. Nakasuji, *Inorg. Chem.*, 2001, **40**, 5476–5478.
60 T. Yamamoto, T. Uemura, A. Tanimoto and S. Sasaki, *Macromolecules*, 2003, **36**, 1047–1053.
61 D. T. Walker, C. D. Douglas and B. J. MacLean, *Can. J. Chem.*, 2009, **87**, 729–737.
62 (*a*) Y. Y. Bao, Q. B. Li, B. Liu, F. F. Du, J. Tian, H. Wang, Y. X. Wang and R. K. Bai, *Chem. Commun.*, 2012, **48**, 118–120; (*b*) T. S. Wang, N. Zhang, R. K. Bai and Y. Y. Bao, *J. Mater. Chem. C*, 2018, **6**, 266–270; (*c*) Y. Y. Bao, T. S. Wang, Q. B. Li, F. F. Du, R. K. Bai, M. Smet and W. Dehaen, *Polym. Chem.*, 2014, **5**, 792–798; (*d*) Y. Y. Bao, H. Wang, Q. B. Li, B. Liu, Q. Li, W. Bai, B. K. Jin and R. K. Bai, *Macromolecules*, 2012, **45**, 3394–3401; (*e*) T. S. Wang, N. Zhang, Q. B. Li, Z. L. Li, Y. Y. Bao and R. K. Bai, *Sens. Actuators, B*, 2016, **225**, 81–89.
63 H. M. Zhang, X. G. Yan, J. Zhao, X. L. Yang, Z. Huang, G. J. Zhou and Y. Wu, *RSC Adv.*, 2015, **5**, 88758–88766.
64 T. Geng, C. Zhang, M. Liu, C. Hu, G. F. Chen and J. Mater, *Chem. A*, 2020, **8**, 2820–2826.
65 (*a*) M. Albrecht, M. Fiege and O. Osetska, *Coord. Chem. Rev.*, 2008, **252**, 812–824; (*b*) D. Singh, V. Nishal, S. Bhagwan, R. K. Saini and I. Singh, *Mater. Des.*, 2018, **156**, 215–228; (*c*) Y. Q. Sun, Y. L. Lei, J. Gao, X. H. Sun, S. H. Lin, Q. L. Bao, Q. Liao, S. T. Lee and L. S. Liao, *Chem. Commun.*, 2014, **50**, 10812–10814; (*d*) R. F. Wang, Y. L. Cao, D. Z. Jia, L. Liu and F. Li, *Opt. Mater.*, 2013, **36**, 232–237.
66 (*a*) H. Tong, L. X. Wang, X. B. Jing and F. S. Wang, *Macromolecules*, 2002, **35**, 7169–7171; (*b*) H. P. Diao, L. X. Guo, W. Liu and L. H. Feng, *Spectrochim. Acta, Part A*, 2018, **196**, 274–280.
67 T. Iijima and T. Yamamoto, *Macromol. Rapid Commun.*, 2004, **25**, 669–672.
68 T. Yasuda and T. Yamamoto, *Macromolecules*, 2003, **36**, 7513–7519.
69 T. Iijima, S. I. Kuroda and T. Yamamoto, *Macromolecules*, 2008, **41**, 1654–1662.

70 (*a*) Y. Deng, W. P. Niu, Z. J. Wang and L. H. Feng, *Sens. Actuators, B*, 2017, **238**, 613–618; (*b*) G. He, N. Yan, H. Cui, T. H. Liu, L. P. Ding and Y. Fang, *Macromolecules*, 2011, **44**, 7096–7099.

71 (*a*) L. H. Feng, Y. Deng, X. J. Wang and M. G. Liu, *Sens. Actuators, B*, 2017, **245**, 441–447; (*b*) Y. Bao, B. Liu, H. Wang, J. Tian and R. Bai, *Chem. Commun.*, 2011, **47**, 3957–3959; (*c*) F. Du, H. Wang, Y. Bao, B. Liu, H. Zheng and R. Bai, *J. Mater. Chem.*, 2011, **21**, 10859–10864; (*d*) Y. Bao, B. Liu, H. Wang, F. Du and R. Bai, *Anal. Methods*, 2011, **3**, 1274–1276; (*e*) Y. Bao, B. Liu, F. Du, J. Tian, H. Wang and R. Bai, *J. Mater. Chem.*, 2012, **22**, 5291–5294; (*f*) Y. Bao and R. Bai, *Prog. Chem.*, 2013, **25**, 288–295; (*g*) P. Chen, W. Bai and Y. Bao, *J. Mater. Chem. C*, 2019, **7**, 11731–11746.

72 (*a*) G. Accorsi, A. Listorti, K. Yoosaf and N. Armaroli, *Chem. Soc. Rev.*, 2009, **38**, 1690–1700; (*b*) P. Alreja and N. Kaur, *RSC Adv.*, 2016, **6**, 23169–23217.

73 (*a*) H. Li, S. J. Zhang, C. L. Gong, Y. F. Li, Y. Liang, Z. G. Qi and Z. Y. Wu, *Synth. Met.*, 2014, **198**, 225–229; (*b*) C. G. Wu, H. C. Lu, L. N. Chen and Y. C. Lin, *J. Polym. Sci., Part A: Polym. Chem.*, 2008, **46**, 1586–1597.

74 T. Yasuda, I. Yamaguchi and T. Yamamoto, *Adv. Mater.*, 2003, **15**, 293–296.

75 X. Q. Liu, X. Zhou, X. Shu and J. Zhu, *Macromolecules*, 2009, **42**, 7634–7637.

76 (*a*) T. T. Wang, H. Y. Wang, G. W. Li, M. W. Li, Z. S. Bo and Y. L. Chen, *Macromolecules*, 2016, **49**, 4088–4094; (*b*) M. J. Wu, Y. Han, B. Wang, Y. Yuan, C. F. Xing and Y. L. Chen, *ACS Appl. Bio Mater.*, 2018, **1**, 473–479.

77 Y. Y. Bao, H. D. Keersmaecker, S. Corneillie, F. Yu, H. Mizuno, G. F. Zhang, J. Hofkens, B. Mendrek, A. Kowalczuk and M. Smet, *Chem. Mater.*, 2015, **27**, 3450–3455.

78 (*a*) Y. N. Hong, J. W. Y. Lam and B. Z. Tang, *Chem. Soc. Rev.*, 2011, **40**, 5361–5388; (*b*) J. Mei, N. L. C. Leung, R. T. K. Kwok, J. W. Y. Lam and B. Z. Tang, *Chem. Rev.*, 2015, **115**, 11718–11940; (*c*) R. R. Hu, N. L. C. Leung and B. Z. Tang, *Chem. Soc. Rev.*, 2014, **43**, 4494–4562; (*d*) A. J. Qin, J. W. Y. Lam and B. Z. Tang, *Prog. Polym. Sci.*, 2012, **37**, 182–209; (*e*) Y. Y. Bao, E. Guegain, V. Nicolas and J. Nicolas, *Chem. Commun.*, 2017, **53**, 4489–4492; (*f*) Y. Y. Bao and J. Nicolas, *Polym. Chem.*, 2017, **8**, 5174–5184; (*g*) Y. Y. Bao, E. Guegain, J. Mougin and J. Nicolas, *Polym. Chem.*, 2018, **9**, 687–698.

79 (*a*) S. Y. Shao, J. Hu, X. D. Wang, L. X. Wang, X. B. Jing and F. Wang, *J. Am. Chem. Soc.*, 2017, **139**, 17739–17742; (*b*) J. Hu, Q. Li, X. Wang, S. Shao, L. Wang, X. Jing and F. Wang, *Angew. Chem., Int. Ed.*, 2019, **58**, 8405–8409; (*c*) C. M. Tonge and Z. M. Hudson, *J. Am. Chem. Soc.*, 2019, **141**, 13970–13976.

80 (*a*) A. E. Nikolaenko, M. Cass, F. Bourcet, D. Mohamad and M. Roberts, *Adv. Mater.*, 2015, **27**, 7236–7240; (*b*) Y. J. Xie and Z. Li, *J. Polym. Sci., Part A: Polym. Chem.*, 2017, **55**, 575–584; (*c*) J. C. Rao, X. R. Liu, X. F. Li, L. Q. Yang, L. Zhao, S. M. Wang, J. Q. Ding and L. X. Wang, *Angew. Chem., Int. Ed.*, 2020, **59**, 1320–1326.

81 (*a*) Y. Y. Bao, T. Boissenot, E. Guegain, D. Desmaele, S. Mura, P. Couvreur and J. Nicolas, *Chem. Mater.*, 2016, **28**, 6266–6275; (*b*) S. Matoori, Y. Y. Bao, A. Schmidt, E. J. Fischer, R. Ochoa-Sanchez, M. Tremblay, M. M. Oliveira, C. F. Rose and J. C. Leroux, *Small*, 2019, 1902347; (*c*) A. C. Schmidt, E. R. Hebels, C. Weitzel, A. Kletzmayr, Y. Y. Bao, C. Steuer and J.-C. Leroux, *Adv. Sci.*, 2020, 1903697.

